Title

Why diversity (sometimes) limits disease risk: Drivers underlying diversity-disease relationships in natural and model plant-fungal systems

Permalink

https://escholarship.org/uc/item/9s6553pp

Author

Rosenthal, Lisa Micaela

Publication Date

2021

Peer reviewed|Thesis/dissertation

Why diversity (sometimes) limits disease risk: Drivers underlying diversity-disease relationships
in natural and model plant-fungal systems

By

LISA M. ROSENTHAL

DISSERTATION

Submitted in partial satisfaction of the requirements for the degree of

DOCTOR OF PHILOSOPHY

in

Ecology

in the

OFFICE OF GRADUATE STUDIES

of the

UNIVERSITY OF CALIFORNIA

DAVIS

Approved:

_____
David M. Rizzo, Chair

_____
Felicia Keesing

_____
Andrew M. Latimer

Committee in Charge

2021

Acknowledgements

Of course I am also indebted to the people who supported me in the years approaching graduate school. Thank you to my parents, siblings, niece and nephew, and grandparents for the support and desire to pursue higher education. Thank you to Tom Bruns for a charismatic introduction into the world of fungi.

To my community of friends, thank you for keeping it silly and fun. I am happy to have maintained many lasting friendships from Davis, Sacramento, and the East Bay. In particular, thanks to the lively people from the Farmhouse and Kingman. You know who you are and how much I love you! Extra shoutout to my climbing dirtbags and gymrats. You are great and keep me stoked.

And the rocks of California–Cookie Cliff, Sugarloaf, Snowshed to name a few favorites. Their beautiful, aesthetic granite lines beckon me to spend my free time in the mountains. Although they may bring me heartbreak at times, I'll keep coming back for intense moments of pure joy.

Above all, I am lucky to be supported by my two best friends: Lobster and Corey Todd. To Lobby–you bring me calm and happiness. Whenever I need a break from work, you're there to snuggle, follow me to the kitchen, and will listen to me say (for the millionth time) that you're such a good boy. And Corey, you're my favorite person and biggest role model. You balance me out and keep me grounded. I couldn't ask for a better person to have been by my side for all of these past years and years to come.

Abstract

Global losses of biodiversity alter interactions amongst hosts and pathogens, and in turn, affect disease dynamics. Uncovering the mechanisms underlying relationships between diversity and disease risk is essential for predicting and managing emerging outbreaks. It is also critical to assess how decisions that researchers make, such as how to measure disease risk, affect inference in diversity-disease patterns. In my dissertation, I broadly sought to understand why diversity (sometimes) limits disease risk by focusing on two pathosystems.

The first system I examined is a forest disease sudden oak death, caused by *Phytophthora ramorum*, a generalist oomycete pathogen that has killed millions of tanoak and oak trees along the coast of California and southwestern Oregon. Studying the biology of natural disease systems is powerful for understanding linkages among community composition, host competence (i.e. the ability to acquire infections and contribute to transmission), and various metrics of disease. In chapter 1, I quantified the sporulation potential of common plant species inhabiting the Big Sur region of coastal California. These lab-based competence assays indicated that bay laurel and tanoak produced large quantities of sporangia; all remaining species produced much less. In chapter 2, I studied natural forests infested by sudden oak death to empirically evaluate hypotheses underlying previously observed negative diversity-disease relationships (i.e. 'dilution effect'). In order to understand how the whole host community might contribute to transmission risk, I leveraged data from the sporulation assays and augmented it to plant community and disease field data from a large forest monitoring plot network. I demonstrated that aggregating disease observations at the community-level can lead to misinterpretations of dilution mechanisms, bias towards a negative diversity-disease relationship, and through review of the dilution effect literature, I found that this oversight is surprisingly common.

I also relied on a tractable model system consisting of crop seedlings and an agricultural fungal pathogen, *Rhizoctonia solani*. In chapter 3, I planted and inoculated experimental mesocosms in a greenhouse to test how variation in overall species densities and species loss order along a richness gradient affects disease risk. Consistent with theoretical expectations, richness only limited disease when species loss order negatively correlated with host competence and overall species density

remained constant with richness. When species density positively correlated with richness or species loss order was random, richness had either a positive or negligible association with disease.

Returning to my overarching question, I found that diversity is more likely to limit disease risk under specific patterns of community assembly and when disease risk is measured as community prevalence. These results present areas ripe for continued research, such as documenting how communities naturally (dis)assemble. They also raise points for discussion, including whether community prevalence–which captures overall disease burden rather than risk of acquiring disease–should be considered under the dilution effect purview. This work adds to the rich and rapidly progressing research focused on uncovering *why* biodiversity alters disease dynamics.

Contents

Chapter 1. Sporulation potential of *Phytophthora ramorum* differs among common California plant species in the Big Sur region

Lisa M. Rosenthal[1,2], Sebastian N. Fajardo[2], David M. Rizzo[2]

[1] Graduate Group in Ecology, University of California, Davis, CA 95616, USA

[2] Department of Plant Pathology, University of California, Davis, CA 95616, USA

Abstract

Sudden oak death (SOD), caused by the generalist pathogen *Phytophthora ramorum*, has profoundly impacted California coastal ecosystems. SOD has largely been treated as a two-host system, with *Umbellularia californica* as the most transmissive host, *Notholithocarpus densiflorus* less so, and remaining species as epidemiologically unimportant. However, this understanding of transmission potential primarily stems from observational field studies rather than direct measurements on the diverse assemblage of plant species. Here, we formally quantify the sporulation potential of common plant species inhabiting SOD-endemic ecosystems on the California coast in the Big Sur region. This study allows us to better understand the pathogen's basic biology, trajectory of SOD in a changing environment, and how the entire host community contributes to disease risk. Leaves were inoculated in a controlled laboratory environment and assessed for production of sporangia and chlamydospores, the infectious and resistant propagules, respectively. *P. ramorum* was capable of infecting every species in our study and almost all species produced spores to some extent. Sporangia production was greatest in *N. densiflorus* and *U. californica* and the difference was insignificant. Even though other species produced much less, quantities were non-zero. Thus, additional species may play a previously unrecognized role in local transmission. Chlamydospore production was highest in *Acer macrophyllum* and *Ceanothus oliganthus*, raising questions about the role they play in pathogen persistence. Lesion size did not consistently correlate with the production of either sporangia or chlamydospores. Overall, we achieved an empirical foundation to better understand how community composition affects transmission of *P. ramorum*.

Introduction

Emergent diseases operate in dynamic and complex ecological communities of multiple interacting hosts and pathogens (Johnson *et al.* 2015b). The vast majority of human, wildlife, and plant diseases are caused by multi-host pathogens (Woolhouse 2001) and as a result, control strategies often require detailed knowledge about many host-pathogen interactions. Gathering information on host susceptibility and infectiousness (i.e., host competency) is important in order to inform targeted strategies for management in new or changing environments.

Sudden oak death (SOD) is a prominent forest disease caused by the generalist invasive oomycete pathogen Phytophthora ramorum, which has profoundly impacted California coastal ecosystems since its initial observations in the mid-1990s (Garbelotto *et al.* 2003; Rizzo & Garbelotto 2003). Symptoms can develop as lethal canker infections, primarily on tanoak (*Notholithocarpus densiflorus*) and a subset of true oak species (*Quercus* spp.), and nonlethal foliar and twig lesions (Rizzo *et al.* 2005). Field measurements among three dominant species showed that bay laurel (*Umbellularia californica*) produced the greatest concentration of *P. ramorum* inoculum in the form of infectious sporangia, tanoak produced significantly fewer, and no sporangia were recovered from coast live oak (*Quercus agrifolia*) (Davidson *et al.* 2005, 2008). Naturally infected redwood (*Sequoia sempervirens*) foliage was incubated in the laboratory and found to occasionally produce sporangia, but the concentrations were not quantified (Davidson *et al.* 2008). Although tests for sporulation on additional California species have not been published, field observations suggested other common plant species either contribute very little or not at all to transmission (Meentemeyer *et al.* 2004; Grünwald *et al.* 2019). Thus, SOD has largely been treated as a two-host system, with bay laurel being the most transmissive host, tanoak less so, and all remaining species as noninfectious. This conventional knowledge has formed the foundation for disease risk maps (Meentemeyer *et al.* 2008a), management plans (Cobb *et al.* 2013, 2017), and many ecological studies (e.g. Cobb *et al.* 2010, 2012b; Dillon & Meentemeyer 2019).

The goal of this study is to formally quantify the inoculum-production potential of common *P. ramorum* hosts from California coastal forests. While much has been learned about the disease in the absence of such a comprehensive survey, we are motivated for several reasons. First, we are filling in the gaps of the pathogen's basic biology. Multiple studies have already assessed the

competencies of host species outside of California due to the pathogen's potential to cause epidemics in new locations (Linderman & Davis 2007; Hüberli *et al.* 2008; Tooley & Browning 2009; Jinek *et al.* 2011; Ireland *et al.* 2012; Harris & Webber 2016), but the same has yet to be done for the region most severely affected by the disease.

Quantifying sporulation potentials also allows us to understand more about the trajectory of SOD in a changing environment. In addition to possible genetic changes in the pathogen, variation in either host or climatic variables will influence its epidemiology. For example, increased fuel loads created by SOD-induced mortality interact with wildfires to increase fire severity (Metz *et al.* 2011). This leads to increased mortality of aboveground stems (Metz *et al.* 2013) and belowground genets (Simler *et al.* 2018), but also increased opportunity for sexual regeneration for some species in a forest dominated by asexually reproducing species (Simler-Williamson *et al.* 2019). The fire-disease interaction presents an interesting opportunity for compositional shifts to take place in novel gaps. Moreover, climate change is expected to shift the geographic ranges of host species, as well as alter the distribution of landscapes with favorable growth conditions for the pathogen (Meentemeyer *et al.* 2011). Overall, uncertainty in the future's forest composition and the distribution of the pathogen provokes newfound reason to understand the sporulation potential of species beyond what is conventionally understood.

Finally, this study will generate a more nuanced perspective of how the entire host community may contribute to disease risk. Current epidemiological models have typically only considered bay laurel and tanoak as transmissive hosts (Ndeffo Mbah & Gilligan 2010; Cobb *et al.* 2012a). These models are highly sensitive to minor increases in inoculum load (Cobb et al. 2012), implying that undetected low-competency hosts may undermine optimal management strategies (Ndeffo Mbah & Gilligan 2010). The role of non-host species must also not be disregarded; after accounting for the densities of bay laurel and tanoak, more diverse plant communities were associated with a lower probability of SOD infection (Haas *et al.* 2011, 2015). The mechanisms driving a negative relationship between diversity and disease risk are highly debated and speculated about (Johnson *et al.* 2015a; Halsey 2019; Rohr *et al.* 2020), but one suggestion is that non-host species may lower transmission by reducing encounter rates between infected and susceptible individuals (Keesing *et al.* 2006). Data on sporulation potential can leverage nearly two decades of ecological data, making

SOD an ideal model system to elucidate mechanisms driving the disease-diversity relationship involving a forest pathogen.

This study assesses the sporulation potential of common plant species inhabiting SOD-endemic ecosystems on the California coast. The intent of this study is to estimate the interspecific variation in sporulation potential. In order to control for phenological differences that would manifest in a state-wide survey (Dodd *et al.* 2008), we focused our sampling efforts on the Big Sur region, where we use a network of 280 long-term monitoring plots to identify the top 10 most common plant species in both redwood and mixed evergreen forests (Metz *et al.* 2011, 2012). Leaf tissue from each species was inoculated in a controlled laboratory environment and assessed for production of its two spore types, sporangia and chlamydospores. Sporangia and their released zoospores are the pathogen's infectious propagules and thick-walled chlamydospores might facilitate long-term survival in the soil (Fichtner *et al.* 2007), but consensus on their epidemiological role is still unclear. Specifically, we address the following questions: i) How do plant species vary in sporangia and chlamydospore production? ii) Is lesion area positively correlated with spore production?

Materials and Methods

Field sampling

The forests in Big Sur broadly split into two types, one comprised of mixed evergreen species and the other with a similar composition but dominated by redwood (Metz *et al.* 2012). The three most common species in mixed evergreen forests are bay laurel, coast live oak, and tanoak; in redwood forests they are redwood, tanoak, and bay laurel (Metz *et al.* 2012). We inoculated leaf tissue from the top 10 most ubiquitous plant species in our plot network (measured as number of plots in which each species occurs) for both forest types (Table 1.1). Plant samples were collected in the Big Sur area from Landels-Big Creek Reserve (36.070°N, 121.599°W) and nearby private property in May and early June 2019, the seasonal period with greatest sporulation (Davidson *et al.* 2005, 2008). For each species, we collected healthy-looking, fully flushed leaves from 32 individuals. They were rinsed with deionized water, placed in moist plastic bags inside of a cooler, and refrigerated overnight. Inoculations were conducted the following day using *P. ramorum* isolate

4

Table 1.1: Most common plant species from mixed evergreen and redwood forests. Rank values are based off of the number of plots each species is present in (in parentheses). *Since *U. california* and *N. densiflorus* were used in the leaf disc and leaf dip assay, species codes for samples from the detached leaf dip assay are UMCA-D and LIDE-D, respectively.

Species name	Species code*	Common name	Mixed evergreen rank	Redwood rank
Umbellularia california	UMCA or UMCA-D	Bay laurel	1 (116)	3 (68)
Quercus agrifolia	QUAG	Coast live oak	2 (101)	7 (12)
Notholithocarpus densiflorus	LIDE or LIDE-D	Tanoak	3 (83)	2 (86)
Arbutus menziesii	ARME	Madrone	4 (73)	5 (18)
Quercus parvula	QUPA	Shreve's oak	5 (56)	4 (26)
Quercus chrysolepis	QUCH	Interior live oak	6 (52)	14 (2)
Toxicodendron diversilobum	TODI	Poison oak	7 (35)	9 (8)
Heteromeles arbutifolia	HEAR	Toyon	8 (29)	12 (4)
Ceanothus oliganthus	CEOL	Ceanothus	9 (25)	8 (10)
Pinus ponderosa	PIPO	Ponderosa pine	10 (16)	NA (0)
Sequoia sempervirens	SESE	Redwood	21 (5)	1 (111)
Acer macrophyllum	ACMA	Bigleaf maple	13 (11)	6 (14)
Pseutotsuga menziesii	PSME	Douglas fir	18 (6)	10 (6)

PR979 (GenBank accession MN783356), which was originally isolated in 2012 from a bay laurel tree located within the plot network.

Experimental design

Separate experiments were conducted for the broadleaf and conifer species in May and June, respectively. We inoculated leaf discs cut with a cork borer (size 9, 1.25 cm diameter) from broadleaf species (Widmer 2015), but since cutting discs from conifer needles is not possible, entire shoots or needles were inoculated using a detached leaf dip method (Denman *et al.* 2005). For the broadleaf species, 2 leaf discs from each of the 32 individuals were inoculated and quantified for either sporangia or chlamydospores. An additional 2 leaf discs cut from 10 or 32 individuals were used as controls (32 controls were used for tanoak, oak species, and bay laurel; 10 controls were used for all other species). Controls were inoculated with sterile water and spores were quantified to assess presence of naturally occurring *Phytophthora* species. In order to limit intra-individual

variation, all leaf discs from an individual were cut from the same leaf when possible. For the conifer species, 2 shoots or needle fascicles from 32 individuals were inoculated with either sporangia or sterile water and the replicates were subsequently sampled for both sporangia and chlamydospore counts.

While it is more difficult to directly compare species responses from different assays, we decided to inoculate the majority of species using leaf discs because we were more able to limit sampling and methodological error. The leaf disc assay allowed us to scale up replication, which was necessary to detect statistically significant differences among many species, and inoculum was more consistently applied on the flat leaf discs. We attempted to compare results from the two inoculation methods by also performing the leaf dip assays on 10 individuals of bay laurel and tanoak. Overall, leaves from 317 and 106 individuals were used in the leaf disc and leaf dip assays, respectively.

Inoculations

To produce inoculum, the *P. ramorum* isolate was passaged through a rhododendron leaf to ensure pathogenicity and grown on 20% unclarified V8 agar for 7 days at $20°$C under natural light. Cultures were flooded with sterile water and incubated under the same conditions. After 48 h, we scraped the colonies to dislodge the sporangia. Sporangia suspensions were rinsed with sterile water and filtered with 4-ply cheesecloth. The concentration was estimated with a hemocytometer and adjusted to 4,000 sporangia/ml (Tooley & Browning 2009).

Following a modified protocol from Widmer (2015), leaf discs were placed into quartered Petri dishes and 15 μl of inoculum was pipetted onto the underside surface. In order to maintain high relative humidity, the Petri dishes were closed with lids lined with sterilized Whatman No. 1 filter paper dampened with 150 μl of sterile water and placed inside of moist clear plastic containers. The leaf discs were incubated under natural light at $20°$C, and were removed after 5 days for quantification of sporangia, chlamydospores and lesion area. In order to estimate a minimum baseline of sporangia originating from the inoculum source alone, we also incubated 8 drops of the sporangia solution without a host.

Detached leaves were held at the petioles, submerged in inoculum to a depth of 4 cm for 30

s, and placed inside a moisture chamber with the underside down (Denman *et al.* 2005). Each chamber contained 6–12 leaves of the same treatment depending on available space. Leaves sat on a sterilized metal mesh platform contained in clear plastic containers lined with moist paper towels. The leaves were incubated under the same conditions as the leaf discs for 5 days. After 48 h, we gently rinsed the control and treatment leaves with running distilled water to ensure that recovered sporangia were produced post-inoculation, rather than from residual inoculum.

Assessments of lesion area and spore production

We estimated lesion area by photographing the underside of all of the leaf discs and measuring the area of visible necrosis with the software program ImageJ (v10.2, National Institutes of Health, USA). We counted sporangia by selecting half of the samples, adding 100 ul of water to each disc and scraping with the flat side of a flame-sterilized T-pin 20 times on the underside and 10 times on the topside (modified from Ireland *et al.* 2012). We pipetted the dislodged sporangia into 0.2 ml strip tubes, added 2.5 μl of lactophenol cotton blue (LPCB) solution, a killing agent and fungal preservant, and stored at 4°C for up to 3 months. Estimating sporangia production involved adding 5 μl of well-mixed sporangia solution onto a slide, counting all of the sporangia under a compound microscope, and repeating for a total of 3 times. The remaining half of the leaves were used for chlamydospore quantification. Since chlamydospores are typically embedded within the leaf tissue, we counted them directly on the leaves. The leaf discs were placed into 2 ml tubes of 1 M potassium hydroxide (KOH), which makes the leaf tissue transparent, and stored at room temperature for 2–4 weeks before counting under the compound microscope (Fichtner *et al.* 2007, 2009). For leaves with large quantities of chlamydospores (i.e. >200 spores), we used the micrometer in the microscope eyepiece reticle as a transect to sample a smaller proportion.

In order to process the leaves from the leaf dip assay in a similar manner, from the inoculated regions we randomly removed 6 needles from redwood and Douglas fir (*Pseudotsuga menziesii*) shoots, 2 out of 3 needles from ponderosa pine (*Pinus ponderosa*), and cut 2 leaf discs with the cork borer from bay laurel and tanoak. Photos were taken for assessments of lesion area. As described above, we added 100 μl of water to half of these samples, scraped the leaves, and collected the sporangia solution. Similarly, we added the other half of the samples to 2 ml tubes filled with KOH

for chlamydospore counting.

Viability of the pathogen

In order to test the viability of the pathogen and detect any latent infections, for each species-treatment group, we attempted to reisolate viable *P. ramorum* sporangia and mycelia from up to two replicates of symptomatic and asymptomatic leaves (delineated by presence or absence of visible lesions). Several species in the control group had no samples with lesions; conversely, many inoculated species exclusively had samples with lesions. To test sporangia viability, we dropped 10 μl of sporangia suspension onto oomycete-selective medium PARP (pimaricin-ampicillin-rifampicin-pentachloronitrobenzene agar, Jeffers & Martin 1986) before adding LPCB. Using these same samples, we tested viability of mycelia by plating leaf tissue that was surface sterilized for 30 s in 10% bleach and rinsed in sterile water. We considered samples with recovered cultures to be successfully infected by a viable isolate. Plates were incubated at 20°C in the dark and monitored for mycelial growth for the following 3 to 4 days.

Data analysis

To analyze how the production of sporangia differed among species, we used separate Bayesian generalized linear mixed models for the leaf disc and leaf dip assays. We assumed a Poisson likelihood with a log link function and included species identity as a fixed effect predictor, individual ID as a varying intercept since we subsampled from each individual 3 times for a more accurate estimate, and an offset variable (log-leaf area) to account for differences in leaf area in the leaf dip assay. Although the offset had no effect on the data coming from the leaf disc assay since the discs were equally sized, it allowed us to easily standardize the counts to spores per 1 cm^2.

The chlamydospore counts were overdispersed and, for several species, zero-inflated. Thus, for both of the assays, a series of regular and zero-inflated Poisson and negative binomial models were compared using leave-one-out cross-validation (LOO) (Vehtari *et al.* 2017) and differences were assessed with expected log pointwise predictive density (ELPD) (Vehtari *et al.* 2017). For the leaf disc assay, the best performing model was the zero-inflated negative binomial model with species

8

as a predictor, an offset term (log-area sampled) to correct for different sampling intensities, and species predicting the zero-inflation probability (ΔELPD = -39.3, SE = 7.3). The leaf dip assay model had the same structure, except the zero-inflation probability was predicted by a single intercept (ΔELPD = -2.7, SE = 1.8).

For each of the above models, pairwise contrasts between species intercepts were performed on the models' posterior values. We report mean spore counts by back-transforming the posterior values of the species intercepts, which are in the units of sampled spores per cm^2 per μl. We standardized sporangia counts to total sporangia per cm^2 by multiplying the values by 102.5 μl, the volume of liquid added to the sample. The chlamydospore values did not need additional transformations.

To examine if spore production was associated with lesion area, regressions were run for the two spore types, but data from both assays were included together. For the sporangia regression, predictors included lesion area with slopes and intercepts varying by species, a dummy variable for assay, and individual ID as a varying intercept. The best performing chlamydospore model was a zero-inflated negative binomial model (ΔELPD = -19.9, SE = 7.9). Predictors included lesion area with slopes and intercepts varying by species, a dummy variable for assay, an offset term (log-area sampled), and species predicting the probability of zero-inflation.

All models were performed using `brms` (Bürkner 2017), a package designed to fit Bayesian multilevel models with the programming language `Stan` (Stan Development Team 2019) and was analyzed in the `R` environment (R Core Team 2019). We used weakly informative priors, 4 chains with 4,000 samples per chain (including 2,000 warmup samples), and chain convergence was assessed for each estimated parameter by ensuring Rhat values were less than or equal to 1.01 (Bürkner 2017). Species with spore count values of exclusively 0 were omitted from the analyses since they created convergence issues. Model fits were visually assessed by graphically comparing observed values against posterior predictive draws. Parameters were considered significant when the 90% highest posterior density interval (HPDI) did not cross zero.

Table 1.2: Results of the viability tests for the treatment group only (no viable cultures were recovered from the control group). Species are split by lesion presence (symptomatic and asymptomatic) and viability tests (mycelia and sporangia). Viable mycelia (indicative of infection) and sporangia are denoted by the following symbols: + = presence, - = absence, NA = no sample.

Species	Symptomatic		Asymptomatic	
	Mycelia	Sporangia	Mycelia	Sporangia
ACMA	+	+	NA	NA
ARME	+	+	NA	NA
CEOL	+	-	+	-
HEAR	-	-	-	-
LIDE	+	+	-	+
LIDE-D	+	+	-	-
PIPO	-	-	+	-
PSME	+	-	+	-
QUAG	+	+	NA	NA
QUCH	+	+	+	+
QUPA	+	+	NA	NA
SESE	+	-	+	-
TODI	+	+	+	+
UMCA	+	+	+	+
UMCA-D	+	+	NA	NA

Results

Viability tests

We detected no viable *P. ramorum* mycelia or sporangia in the controls. Most controls had no symptomatic samples, but those that did had lesions caused by non-oomycetes. In contrast, we reisolated viable *P. ramorum* mycelia from all species except for toyon (*Heteromeles arbutifolia*) (Table 1.2). Toyon was found to produce sporangia when inoculated, so it is possible that reisolation methods were not optimized for this species, as was the case for highly infectious larch species in the United Kingdom (Harris & Webber 2016). Most symptomatic samples had both viable mycelia and sporangia, and when there were asymptomatic samples available, many still had viable sporangia. This confirms that *P. ramorum* is capable of producing latent, transmissible infections.

Control samples

Out of 424 control samples in the leaf disc and dip assays, no chlamydospores were found and only low quantities of sporangia were recovered in 2 samples. For these samples, we examined additional subsamples for a total of 9 5-μl counts, and we detected 1 sporangium twice in a bay laurel individual, and 1 sporangium once in a redwood individual. We therefore consider the background levels of *P. ramorum* on our collected leaves to be negligible and all following analyses were performed on the treatment replicates only.

Sporangia and chlamydospore production

Sporangia production differed among host plant species in the leaf disc assay. Some of the variation is attributed to random sampling error since we subsampled from the solutions 3 times, but after accounting for this within-individual variation, we detected strong differences among species (Table A.1, A.2). Bay laurel produced the greatest amount with a median $\pm$ 1 SD of 780 ± 175 sporangia/cm^2, closely followed by tanoak with 526 ± 114. The difference between these two species was not significant. The remaining 8 broadleaf plant species produced significantly fewer sporangia (Figure 1.1). All of these values except for that from madrone (*Arbutus menziesii*) were significantly higher than the estimated number of sporangia contained in the inoculum, indicating that almost all of these species were able to produce non-zero quantities of sporangia.

In the detached leaf assay, bay laurel and tanoak again produced significantly more sporangia than the other species, but they did not significantly differ between each other. On average, tanoak produced more than bay laurel with 264 ± 142 and 164 ± 114 sporangia/cm^2, respectively. These values are about 2 to 4 times lower than those from the leaf disc assay, suggesting that results from the detached leaf assay are relatively lower due to the methodology. Douglas fir and redwood produced similar quantities of sporangia, 70.7 ± 23.9 and 61.2 ± 18.6, respectively. Out of the 96 subsamples from 32 individuals, we detected 1 sporangium from ponderosa pine, which conceivably could have been from residual inoculum that was not washed off after 48 hours. Consequently, we consider the inoculum produced by ponderosa pine to be inconsequential.

Chlamydospore production also varied among plant species (Table A.1), but we were only able

Figure 1.1: Distributions (grey) depict the predicted mean sporangia per cm^2 produced on different plant species. Lines (black) represent the 90th HDPI and point estimate marks the median. The two panels are seperated by assays. A. menziesii (ARME) and the inoculum only control were not significantly different, and neither were N. densiflorus (LIDE) and U. californica (UMCA) in either assay. Additionally, P. ponderosa (PIPO) was not significantly different from zero.

to confidently count spores from 6 broadleaf and 2 conifer species (Figure 1.2). The leaf tissue of the true oak species, bay laurel, and redwood was too sclerotic for the KOH to adequately dissolve, making it difficult to visualize and identify the spores. For those that we could quantify, after accounting for the zero-inflation, the median $\pm$ 1 SD quantity of chlamydospores produced per cm^2 were the following: bigleaf maple (*Acer macrophyllum*, 1510 $\pm$ 330); ceanothus (*Ceanothus oliganthus*, 1290 $\pm$ 287); madrone (51.4 $\pm$ 12.5); poison oak (*Toxicodendron diversilobum*, 98.7 $\pm$ 40.4); tanoak (4.20 $\pm$ 3.00); and toyon with 0 (not included in model). Pairwise differences between these six species were all significant except for between bigleaf maple and ceanothus. In the leaf dip assay, Douglas fir produced 31.0 $\pm$ 13.1, tanoak 1.07 $\pm$ 1.49, and ponderosa pine 0 (not included in model).
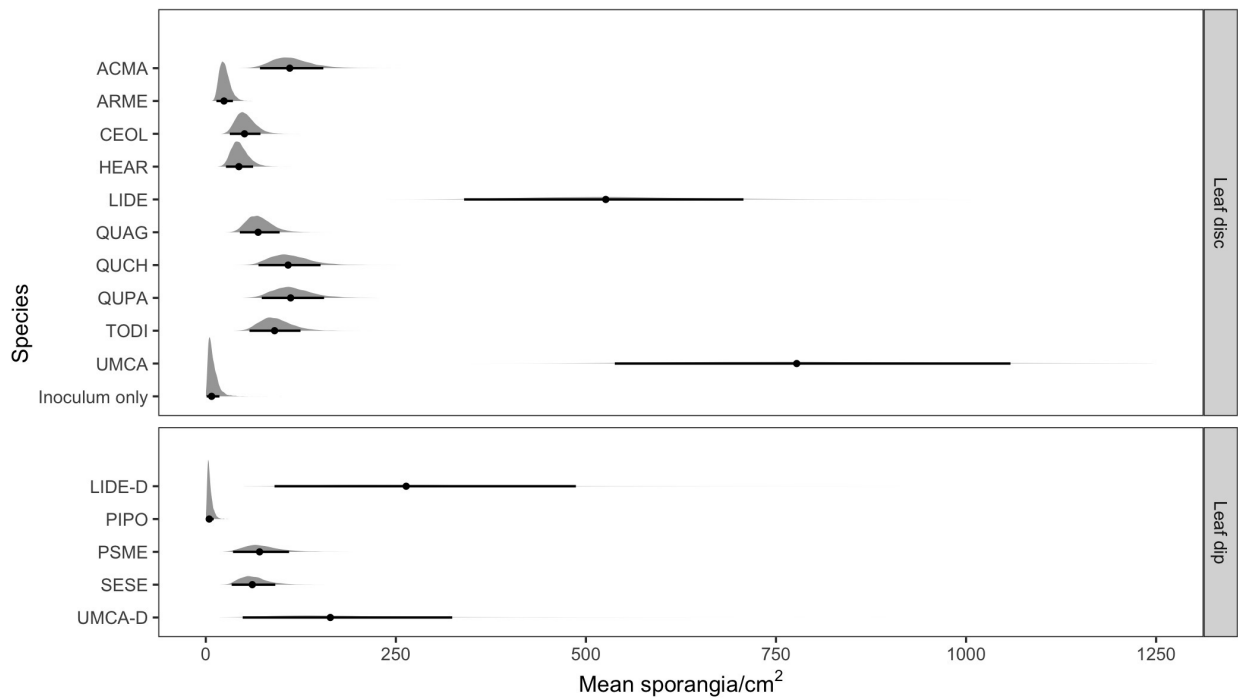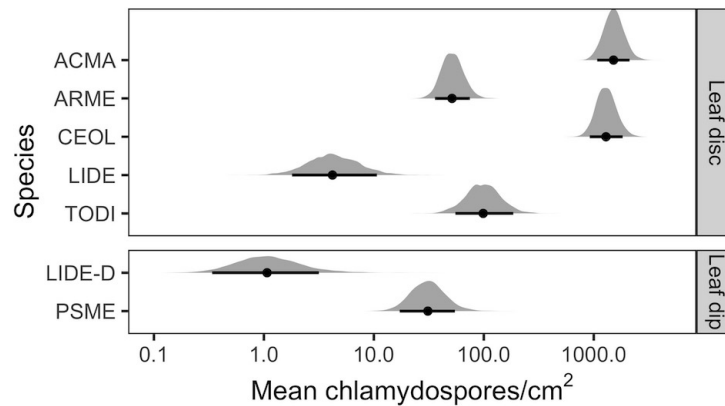

Figure 1.2: Distributions (grey) depict the predicted mean chlamydospores per cm^2 produced on different plant species. Lines (black) represent the 90th HDPI and point estimate marks the median. The two different panels are separated by assays. Pairwise differences between all species were significant except for between A. macrophyllum (ACMA) and C. oliganthus (CEOL).

Spores and lesion size

Except for ceanothus, madrone, and bigleaf maple, mean necrosis encompassed less than 50% of the exposed leaf tissue. The oaks in particular produced the lowest lesion coverages, with a median $\pm$ 1 SD of 7.42 $\pm$ 4.48, 18.5 $\pm$ 14.9, 21.8 $\pm$ 20.0, and 6.82 $\pm$ 9.20 for tanoak, coast live oak, Shreve oak (*Q. parvula*), and interior live oak (*Q. chrysolepis*), respectively. Grouped across all species we detected a significantly positive relationship between sporangia production and lesion area (Table A.3). However, when we examined species-specific relationships, slopes were significantly positive

only for bigleaf maple, interior live oak, poison oak, tanoak (from leaf dip assay) and bay laurel (from leaf dip assay) (Figure 1.3). These findings indicate that for most species, lesion size does not predict sporangia quantity. Likewise, there was a positive relationship between chlamydospores and lesion area across all species (Table A.3), but the species-specific slopes were only significantly positive for bigleaf maple, ceanothus, and poison oak.
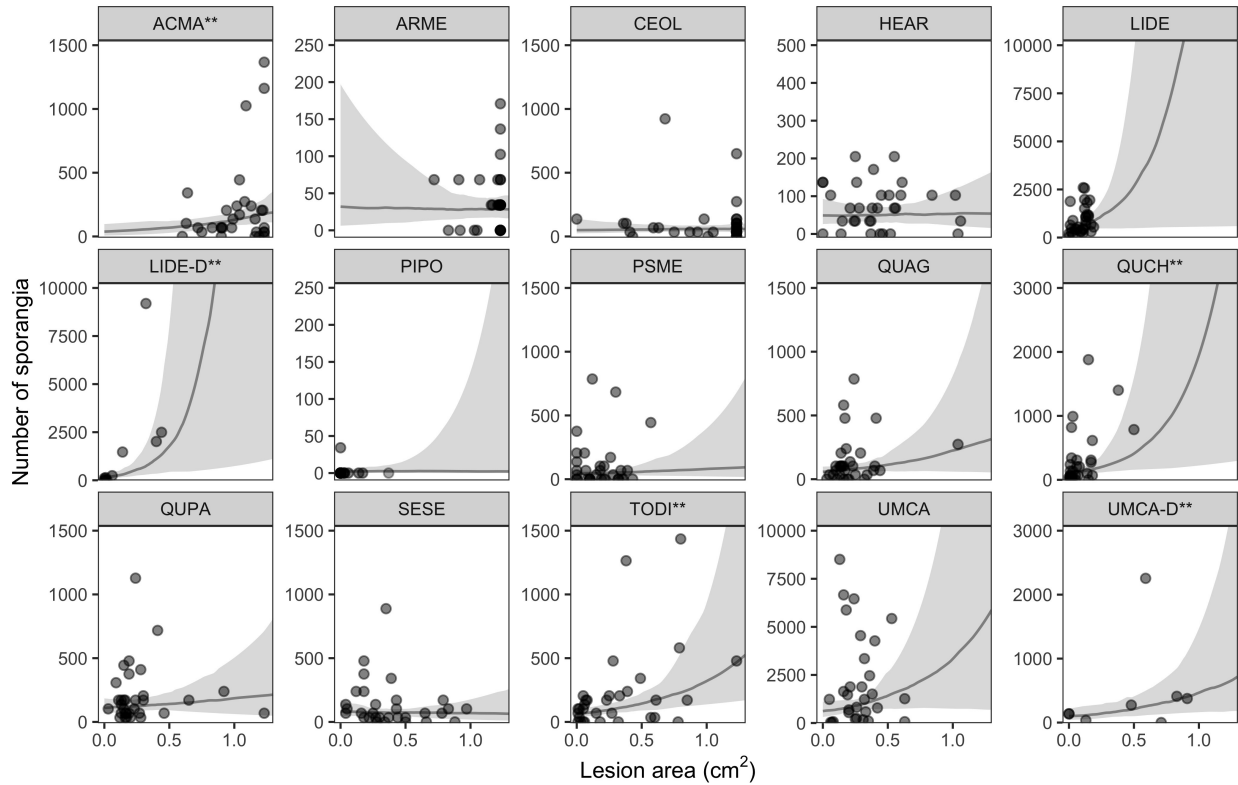
Figure 1.3: The relationship between lesion area (cm^2) and number of sporangia produced across species. Points are mean values grouped by individual and the grey shaded region represents the posterior predictions of the model. **denotes a significant relationship between lesion area and sporangia for that species (90th HDPI of slope coefficient does not cross zero).

Discussion

We found that all host species included in the study support *P. ramorum* infections when challenged, but sporulation potential varies significantly across species. Bay laurel and tanoak were prolific sporangia producers, while the majority of species produced relatively lower amounts of sporangia. Large quantities of chlamydospores were also found in some species. Since our collections were exclusively from the Big Sur region, and natural variability in susceptibility to

P. ramorum has been documented for bay laurel, tanoak, and coast live oak (Dodd *et al.* 2005; Hayden *et al.* 2011; Hüberli *et al.* 2012), it is possible that sporulation values and relative ranks among species may differ should the study be expanded to more populations. In general, our results align closely, but not perfectly, with previous understanding of SOD-infested California coastal ecosystems.

Results from our study suggest the sporulation potential of tanoak and bay laurel are equivalent, but most studies across California regard bay laurel as the primary driver of SOD epidemics (e.g. Cobb *et al.* 2010; Garbelotto *et al.* 2017; Dillon & Meentemeyer 2019). Field measurements indicated bay laurel was capable of producing orders of magnitude more sporangia than tanoak (Davidson *et al.* 2008), and early observational studies also found presence of bay laurel, but not tanoak, was the only significant host predictor in SOD infestations (Swiecki & Bernhardt 2002; Meentemeyer *et al.* 2008b). However, the disease had not yet progressed to the northern parts of California, where tanoak is most abundant. The negative correlation between disease and tanoak distribution may have led to the insignificance of tanoak (Meentemeyer *et al.* 2008b). Meanwhile, subsequent models from field collected data in the Big Sur area and more northern coastal regions suggested that the two species both contribute significantly to the likelihood of SOD infections (Haas *et al.* 2011; Cobb *et al.* 2012a).

We also detected sporangia production in species implicated as epidemiologically unimportant. Generally, true oak species are considered dead-end hosts that are incapable of producing sporangia (Davidson *et al.* 2005), while all other species are considered low-competency hosts at most (Meentemeyer *et al.* 2004). Aside from ponderosa pine and madrone, our study showed that all of the other tested species, including true oak species, were able to produce non-zero quantities of sporangia. Moreover, several hosts abundantly produced chlamydospores, which may or may not be important for pathogen survival. These spores are known to survive at high rates in the soil for the duration of California's dry summer months (Fichtner *et al.* 2007) and although germination rates are low (Tooley *et al.* 2008), large numbers ensure the presence of viable inoculum in the soil and litter. Specifically, bigleaf maple and ceanothus produced quantities of chlamydospores that rival the maximum known concentrations on highly susceptible species, rhododendron and bay laurel (Fichtner *et al.* 2007, 2009).

While we believe species differences within the leaf disc and leaf dip assays may be compared, we caution against direct contrasts between assays. Cutting leaf discs involves additional wounding around the leaf edges, which might contribute to differences in sporulation potential by inducing or suppressing defenses against pathogens. However, we are unaware of studies that have examined how wounding affects local defenses on sporulation; it remains an open area of study. We estimate that species in the leaf dip assay sporulated 2 to 4 times less than species in the leaf disc assay. As a result, the sporulation potentials and lesion areas of Douglas fir and redwood may have been underestimated relative to the broadleaf species and direct comparisons with broadleaved species besides tanoak and bay laurel remain imprecise.

Given that laboratory inoculations are not perfect representations of *in situ* infections, we offer explanations to account for discrepancies between our findings and field-based studies. First, our inoculum concentration, 4000 sporangia/ml, corresponds to the seasonal peak of sporangia production from bay laurel leaves during a wet year (Davidson *et al.* 2008), conditions that exceed average. Increased inoculum loads could lead to artificially higher rates of necrosis, infection, and sporulation (Tooley *et al.* 2004, 2013; Hansen *et al.* 2005), including for species that typically do not show foliar symptoms in nature (Vettraino *et al.* 2008). Furthermore, the inoculated detached leaves and cut leaf discs were without whole plant systemic defenses. While lowered defenses could elevate susceptibility (Orłowska *et al.* 2012) and potentially sporulation, direct comparisons from both leaf discs (Cohen 1993; Brown *et al.* 1999; Kortekamp 2006) and detached leaves (Harrison & Lowe 1989; Brown *et al.* 1999) have shown sporulation and susceptibility rates to strongly correlate with those from intact plants.

It is also conceivable that our sporangia production estimates are not reflective of realized plant-plant transmission due to components of host physiology and phenology. For example, since overstory trees are suspected to have a greater influence on *P. ramorum* establishment and transmission (Metz *et al.* 2012; Peterson *et al.* 2014; Simler-Williamson *et al.* 2021), species in the understory may comparatively transmit the pathogen much less regardless of their sporulation potential. Additionally, deciduous species have a narrower transmission window because their leaves flush out nearly 4–5 months after evergreen species begin producing spores (Davidson *et al.* 2008). Finally, biases inherent in observational plot studies should not be overlooked. Symptoms are most

obvious on common, susceptible, large trees, and for this reason field protocols often rely on bay laurel and tanoak as indicator species to represent the community's infection and mortality rates. Even if all hosts are equally examined for symptoms, our results and others' indicate that detection can be low since *P. ramorum* can cause latent or small lesions (Denman *et al.* 2009; Harris & Webber 2016).

These caveats evoke the need to assess the ecological relevance of our sporulation results by corroborating them with field-collected data. One simple first step would be to update risk maps that rely on sporulation potentials primarily grounded in expert opinion (Meentemeyer *et al.* 2004, 2011; Cunniffe *et al.* 2016) with our empirically-derived sporangia values and assess if model performance improves. Another approach is to explore the explanatory power of community competency (Johnson *et al.* 2013, 2015a), the cumulative product of each tree species' density and measured sporulation potential, for predicting infection risk in a stand. Johnson *et al.* (2013) found community competency and its associated interactions among amphibian hosts explained 89% of the variance in total load of a trematode parasite. Many years of research focus has amassed several rich SOD datasets complete with community and disease data, allowing a similar analysis to be completed in the near future.

Until our results are validated and calibrated with field data, we cautiously speculate on the consequences they might have on our understanding and management of SOD. We reiterate existing calls to thin both bay laurels and tanoaks in stands that are at-risk or recently infested (Valachovic *et al.* 2008; Cobb *et al.* 2013), since they both appear to be significant drivers of pathogen spread. Regarding the implications of low-competency hosts, we hypothesize they play a role in transmission at the local, but not landscape scale. Perhaps the strong performance of the California state-wide risk model from Meentemeyer *et al.* (2008a), which incorporates presence of bay laurel as the only host predictor, speaks to the notion that limited knowledge of one of the key hosts is sufficient to garner a coarse outlook on disease risk. We still suspect pathogen spread involving more minor hosts is occurring, albeit sometimes at low intensities, given that most species produce inoculum either in the form of sporangia or chlamydospores. They may act as reservoirs, facilitating transmission to nearby high-competency hosts, which can lead to more secondary transmission and mortality at the broader scale.

Overall, this study is largely confirmatory, echoing much of what has been suspected regarding host competency, but never formally and exhaustively tested. The greatest value of this study lies in what is now possible. By generating an empirical foundation for host competency, we can better explore how the composition of newly invaded or disturbance-altered communities may interact with the epidemiology of *P. ramorum*. Additionally, we now have an exciting opportunity to test the importance of host community composition on local transmission in an invasive forest pathogen system. This study augments decades of ecological monitoring, positioning sudden oak death as an even more valuable system to explore the community's role in disease dynamics.

Acknowledgements

Chapter 2. Community-level prevalence of a forest pathogen, not individual-level disease risk, declines with tree diversity

Lisa M. Rosenthal[1,2], Allison B. Simler-Williamson[3], David M. Rizzo[2]

[1] Graduate Group in Ecology, University of California, Davis, CA 95616, USA

[2] Department of Plant Pathology, University of California, Davis, CA 95616, USA

[3] Department of Biological Sciences, Boise State University, Boise, ID 83725, USA

Abstract

Understanding why diversity sometimes limits disease is essential for managing outbreaks; however, mechanisms underlying this 'dilution effect' remain poorly understood. Negative diversity-disease relationships have previously been detected in plant communities impacted by an emerging forest disease, sudden oak death. We used this focal system to empirically evaluate whether these relationships were driven by dilution mechanisms that reduce transmission risk for individuals or from the fact that disease was averaged across the host community. We integrated laboratory competence measurements with plant community and symptom data from a large forest monitoring network. Richness increased disease risk for bay laurel trees, dismissing possible dilution mechanisms. Nonetheless, richness was negatively associated with community-level disease prevalence because disease was aggregated among hosts that vary in disease susceptibility. Aggregating observations (which is surprisingly common in other dilution effect studies) can lead to misinterpretations of dilution mechanisms and bias towards a negative diversity-disease relationship.

Introduction

Human-caused biodiversity loss (Cardinale *et al.* 2012) alters interactions among hosts and pathogens with cascading effects on infectious diseases of humans, plants, and wildlife. Susceptible hosts are often hypothesized to be more vulnerable to infections in depauperate communities than

in nearby richer communities, a phenomenon coined the 'dilution effect' (Ostfeld & Keesing 2012; Civitello *et al.* 2015; Magnusson *et al.* 2020). However, the relationship between infection risk and diversity may also be positive (Guilherme Becker & Zamudio 2011), idiosyncratic (Salkeld *et al.* 2013), or context-dependent (Halliday & Rohr 2019; Liu *et al.* 2020). If diversity predictably covaries with factors that limit disease, conservation of biodiversity could be a viable win-win strategy; if not, targeted management of specific species would be needed (Rohr *et al.* 2020). Thus, it is essential to understand why diversity affects disease dynamics to forecast and manage disease outbreaks under global change (Johnson *et al.* 2015a; Rohr *et al.* 2020).

Higher diversity communities may be associated with less disease risk for individuals if they contain species that contribute little to inoculum pressure and reduce transmission risk (Keesing *et al.* 2006). 'Diluter' species might regulate the densities of high-competence hosts, or those that efficiently acquire and transmit pathogens, via competition for finite resources (Fig. 2.1A; Strauss *et al.* 2015). Decreases in diversity have been associated with increases in infections for plant, animal, and zoonotic diseases (Ostfeld & Keesing 2000; Mitchell *et al.* 2002; Johnson *et al.* 2012). Covariance between competent host densities and diversity likely depends on additional relationships among host competence, nestedness, and total density. However, few studies have investigated these linkages thus far (e.g. Johnson *et al.* 2013; Lacroix *et al.* 2014).

The dilution effect may also be driven by richness *per se* (Fig. 2.1B). For example, communities of greater diversity might be associated with less disease if diluter species reduce encounters between infectious and susceptible hosts (e.g. by ingesting propogules; Schmeller *et al.* 2014) or if they lower the likelihood of transmission given an encounter (e.g. by altering microclimates; Zhu *et al.* 2000). Since multiple dilution mechanisms can operate simultaneously, diversity-associated mechanisms driven by encounter/transmission reduction can be deduced after accounting for competent host densities (Strauss *et al.* 2016, 2018).

Furthermore, diversity-disease relationships may change whether disease is measured for particular host individuals or species, or the overall host community (Fig. 2.1C). For instance, individual risk of hantavirus infection in the most susceptible rodent species did not vary across habitats, but seroprevalence of the entire rodent community was greater in rural settings compared to forests (Piudo *et al.* 2011). Differences arise because disease in a focal host controls for
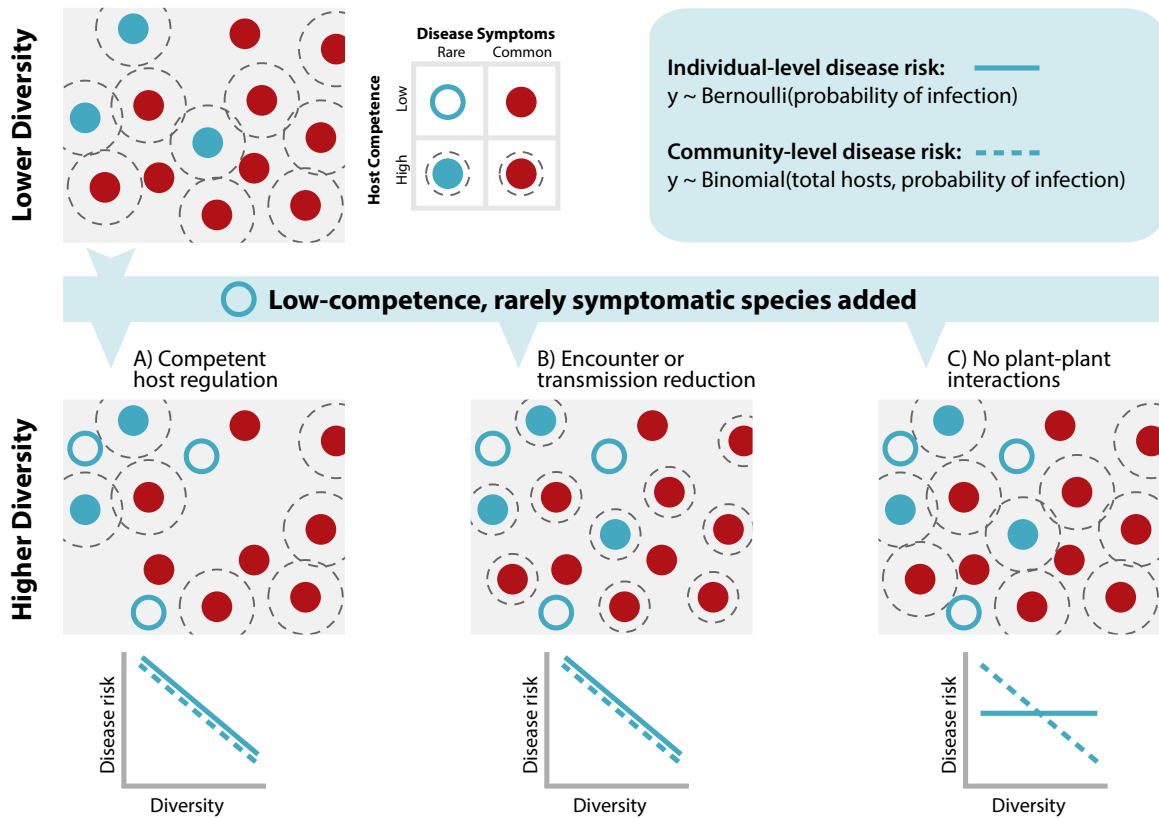
Figure 2.1: Negative diversity-disease relationships assessed at the community level may be affected by multiple dilution mechanisms and/or measurements of disease risk. The addition of low-competence, rarely symptomatic species (i.e. 'diluter' species) to higher diversity communities may potentially limit transmission risk, as measured by average individual-level disease risk, A) by reducing the density of competent hosts ('competent host regulation', modified *sensu* Keesing et al. 2006), or B) by reducing encounter rates or probability of transmission between infectious and susceptible individuals ('encounter reduction' or 'transmission reduction' *sensu* Keesing et al. 2006). The addition of these species may also C) have no effect on plant-plant interactions, resulting in no corresponding change in individual-level disease risk. Across all three scenarios, the overall proportion of commonly symptomatic species is lower in the higher diversity community, causing a negative relationship between diversity and community-level disease risk. The area of the dashed halos represent total potential inoculum pressure exerted by competent hosts.

species-specific susceptibility, whereas community-level prevalence aggregates across species and is sensitive to the average susceptibility of individuals from all species. Unlike individual-level disease risk, community-level prevalence does not measure risk of acquiring infections (it measures disease burden) and is predisposed to decline with diversity due to the mathematical inevitability of adding low- or non-susceptible species to the denominator of prevalence. While the majority of studies discussed within the dilution effect context measure disease risk in a particular host, many focus on community-wide disease. Community-level prevalence comprised *ca.* 11%, 27%, and 15% of studies from dilution effect meta-analyses by Civitello *et al.* (2015), Magnusson *et al.* (2020), and Salkeld *et al.* (2013), respectively (Table B.1). Variation in disease metrics alters diversity-disease relationships (Young *et al.* 2014; Luis *et al.* 2018; Roberts & Heesterbeek 2018). This overlooked distinction between individual- and community-level observations might inflate evidence for dilution effects.

To empirically evaluate dilution mechanisms underpinning the disease-diversity relationship and the influence of aggregation, we studied plant communities impacted by sudden oak death, an emerging forest disease that has killed at least 48 million stems of tanoak (*Notholithocarpus densiflorus*) and oak species (*Quercus* spp.) in coastal California and southwestern Oregon since 1995 (Rizzo & Garbelotto 2003; Cobb *et al.* 2020). The causal agent, *Phytophthora ramorum*, is an invasive oomycete pathogen with a wide host range, though some hosts exhibit symptoms more often than others. Field studies in California suggest that transmission is driven primarily by two species: bay laurel (*Umbellularia californica*) and, to a lesser extent, tanoak (Davidson *et al.* 2005, 2008). Whether other forest plant species also contribute to inoculum pressure via asymptomatic sporulation, reduce transmission success, or have no effect on transmission is unknown.

We combined laboratory competence measurements with high-resolution plant community and disease symptom data from a large network of plots in the Big Sur region of California. In a previous analysis of this field-collected dataset, community-level disease prevalence declined with both plant species richness and Shannon-Wiener diversity index, even after accounting for the densities of known competent hosts, bay laurel and tanoak (Haas *et al.* 2011). Although other species might underly dilution mechanisms, such as 'competent host regulation' (via asymptomatic sporulation) or 'encounter/transmission reduction' (modified *sensu* Keesing *et al.* 2006), it is difficult to assess

without investigating individual-level disease risk. In order to test whether this negative diversity-disease relationship arose from dilution mechanisms, or from the fact that disease was averaged across the community, we tested three hypotheses:

i) The dilution effect is driven by competent host regulation, indicated by decreases in individual- and community-level disease risk with diversity, with associated decreases in competent host density.

ii) The dilution effect is driven by encounter/transmission reduction, indicated by decreases in individual- and community-level disease risk with diversity, which persist after accounting for changes in competent host density.

iii) The negative diversity-disease relationship is a product of how disease is measured, indicated by decreases in community-level, but not individual-level, disease risk with diversity.

Our study explores the empirical foundation linking community composition, competence, and different disease metrics. Understanding these links is essential to predicting where diseases may emerge or decline as a function of global threats to biodiversity.

Methods

Study system

Our study was conducted in redwood and mixed evergreen forest types in the Big Sur region of California. Redwood forests are typified by redwood (*Sequoia sempervirens*) canopies, with bay laurel, tanoak, pacific madrone (*Arbutus menziesii*) and various oak species in the subcanopies. Mixed evergreen forests occupy drier sites and consist of similar species excluding redwood.

In this system, woody plants fell into three categories in regard to *P. ramorum*: 'commonly symptomatic', 'rarely symptomatic', and nonhosts. We considered bay laurel, tanoak, coast live oak (*Quercus agrifolia*), and Shreve oak (*Q. parvula*) to be commonly symptomatic hosts because they accounted for the majority of detected infections. Infected true oaks and tanoaks may develop lethal stem cankers, while bay laurels do not experience disease-induced mortality (Rizzo *et al.* 2005). Infectious propagules (sporangia) formed on foliar and branch lesions are most prolifically

23

produced on bay laurel, followed by tanoak (Davidson *et al.* 2005, 2008), and are very rarely observed on true oaks (Vettraino *et al.* 2008). Infections on other, more rarely symptomatic hosts typically lead to nonlethal foliar and branch lesions.

Plot network design and data collection

In 2006 and 2007, plant community and disease data were collected in 500 m^2 plots established to monitor long-term sudden oak death dynamics (see Metz *et al.* 2011). All woody stems at least 1 cm diameter at breast height were recorded for species identity, live/dead status, and visually assessed for *P. ramorum* symptoms. Plant individuals with any symptomatic live stems were considered diseased. Note that we assessed disease—not infections, opening the possibility that some plants were asymptomatically infected (Denman *et al.* 2009).
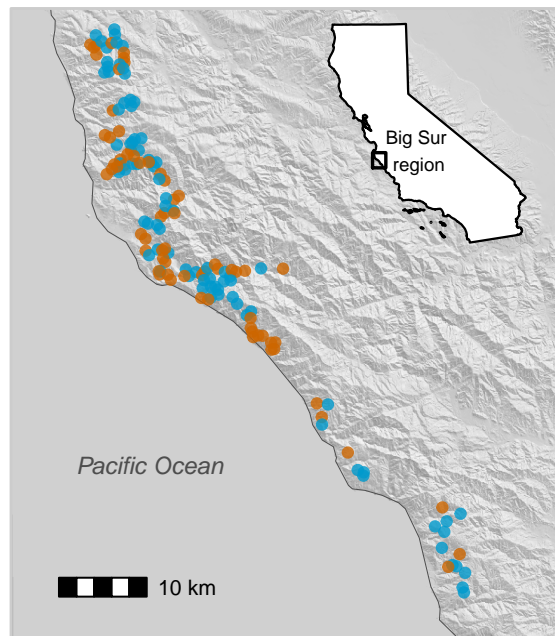
Figure 2.2: Map of 151 study plots located in the Big Sur coastal region of California, USA. Bounding box in the inset state map designates the closeup area. Plots were split among mixed evergreen (blue) and redwood (orange) forest types.

We studied 151 plots where the pathogen was confirmed present using culture-based methods (Fig. 2.2; see Appendix S1 for details, including how our selected plots differed from Haas *et al.* 2011). We adopted host/nonhost categorizations from Haas *et al.* (2011), defined by whether or

not natural infections had been identified on that species (Davidson *et al.* 2003). We measured density of species using total basal area, which better captures variation in tree sizes than counts of individual plants, and the number of individuals, which directly influences community-wide disease prevalence ($\frac{\text{Infected host individuals}}{\text{Total host individuals}}$). Plot diversity was characterized using species richness of woody plants.

To account for other sources of heterogeneity that may correlate with species richness, the same climatic, topographic, and landscape characteristics used by (Haas *et al.* 2011) were estimated for each plot. We used the 30-year mean wet-season precipitation (December–May) calculated from Parameter Elevation Regression on Independent Slopes Model (PRISM; Daly *et al.* 1994); potential solar insolation (PSI; Dubayah & Rich 1995); and the area of host vegetative coverage within 200 m of plot center (Meentemeyer *et al.* 2008b).

Host and community competence

To evaluate how the entire plant community might contribute to overall inoculum pressure, we estimated host competence from the 10 most commonly occurring species in the two forest types (13 species in total; Rosenthal *et al.* in press). In Spring 2019, leaves from 32 individuals per species were collected in the Big Sur region and inoculated with *P. ramorum* in the laboratory. Sporulation was quantified after 5 days of incubation by scraping the leaves, collecting the solution, and counting sporangia under the microscope.

We estimated community competence (K) as the cumulative density of each species weighted by their competence (modified from Johnson *et al.* 2013): $K = \sum_i^S c_i n_i$, where c_i is the mean competence and n_i is the total basal area of species i for S total species per plot. Each species' component contribution to K was calculated as $k_i = c_i n_i$. For species not examined in the competence assay, we assumed missing values were the median of the quantified host competencies. Since these species comprised only 0.7% of the basal area in the dataset, assumptions about their values had a negligible effect.

Statistical Analyses

How density varies with richness

To understand linkages between community composition and disease, we evaluated several measurements of density in relation to plot richness and forest type. Densities of known competent hosts, bay laurel and tanoak, were investigated in separate hurdle models. We predicted the probabilities of their occurrences with a Bernoulli generalized linear model (GLM) and when a species was present in a plot, its basal area was estimated with a gamma GLM. We used a gamma GLM to explore if densities of these hosts could be explained by the relationship between total plant basal area and richness. Additionally, we analyzed the total number of either commonly or rarely symptomatic host plants per plot, using separate negative binomial GLMs.

How community competence varies with richness

To test whether a negative covariance between community competence and richness might explain the past negative diversity-disease relationship, community competence was modeled with a log-normal likelihood and included predictors for plot richness and forest type. A predictable relationship between community competence and diversity is predicated on nested communities. We calculated a nestedness metric based on overlap and decreasing fill (NODF; Almeida-Neto *et al.* 2008) and compared it against 999 null permutations (proportional row and column totals; Strona & Fattorini 2014) using an online software (Strona *et al.* 2014).

How disease risk varies with richness, known competent hosts, and community competence

To address if competent host regulation, encounter/transmission reduction, or aggregation of observations drove the previous negative diversity-disease relationship, we estimated disease risk at the community and individual level. For both hierarchical levels, we contrasted three explanatory models, which included covariates for M1) richness, M2) richness and basal area of tanoak and bay laurel, and M3) richness and community competence. If competent host regulation was a driving mechanism, we expected individual-level disease risk to be negatively associated with richness in

26

M1 and positively associated with either host densities in M2 or community competence in M3. Additionally, if plant species besides tanoak or bay laurel enhanced transmission risk, M3 would have a greater predictive performance than M1 and M2. If encounter/transmission reduction was a contributing factor, we expected to still see a negative effect of richness on individual-level disease risk after incorporating host densities in M2 and/or community competence in M3. Lastly, if the negative diversity-disease relationship was a product of aggregation of observations, we expected to see a negative effect of richness on disease risk at the community, but not individual level.

To isolate how inclusion of rarely symptomatic host species might alter the calculation of community-level disease prevalence, community-wide disease was analyzed both for all hosts (commonly and rarely symptomatic species) and for the four commonly symptomatic host species. Community-level disease prevalence was estimated by modeling I_j, the number of diseased plants in plot j, given n_j, the total number of host plants (j=151 plots). To capture overdispersion in the response variable, we used a beta-binomial likelihood with μ_j, the expected value of probability of disease p_j, and a dispersion parameter θ:

$$I_j \sim \text{Binomial}(n_j,\ p_j)$$
$$p_j \sim \text{Beta}(alpha_j,\ beta_j)$$
$$alpha_j = \mu_j\,\theta \tag{1}$$
$$beta_j = (1 - \mu_j)\,\theta$$
$$logit(\mu_j) = \alpha_0 + BX_j$$

where α_0 is the global intercept and B is a vector of coefficients for the covariates contained in the data matrix X_j. In addition to the covariates mentioned above (richness, host basal areas, and community competence), we incorporated variables for forest type, sample year, precipitation, PSI, and host vegetation in the surrounding landscape in order to control for confounding effects from the sampling design and landscape heterogeneity.

Individual-level disease risk was assessed for the four commonly symptomatic hosts. We modeled I_i, the disease status of individual i of species s located in plot j, using a Bernoulli likelihood with a mean probability p_i (i=4206 individuals from 151 plots and 4 species):

$$I_i \sim \text{Bernoulli}(p_i)$$

$$\text{logit}(p_i) = \alpha_{j[i]} + \alpha_{s[i]} + \beta_{s[i]} richness_{j[i]} + \gamma BA_i$$

$$\alpha_j \sim \text{Normal}(BX_j,\ \sigma_{plot}) \tag{2}$$

$$\begin{bmatrix} \alpha_s \\ \beta_s \end{bmatrix} \sim \text{MVNormal}\Big(\begin{bmatrix} \alpha_0 \\ \bar{\beta} \end{bmatrix},\ \boldsymbol{\Sigma} \Big)$$

where intercept α_j varied by plot, intercept α_s and the effect of richness β_s varied by species, and γ characterized the basal area of the plant (summed among live stems) in order to account for size-dependent variation in susceptibility. Plot-varying intercepts were normally distributed with a mean BX_j, defined by the same predictor variables as described previously in the community-level models. α_s and β_s were drawn from a multivariate normal distribution, defined by means α_0 and $\bar{\beta}$ and covariance matrix Σ.

Host densities and community competence were square root transformed to spread the right-skewed distributions. All variables were centered and scaled by dividing by 2 SD (Gelman 2008). Collinearity was assessed by confirming that correlations between continuous variables were <0.5 (Figure B.1). We contrasted model predictive performance by computing approximate leave-one-out cross-validation, comparing models based on the difference in expected log pointwise predictive density (ELPD; Vehtari *et al.* 2017). We tested for spatial autocorrelation using a Moran's I correlogram on the mean residuals from the best performing community-level disease prevalence including all hosts. No significant spatial clustering emerged (Figure B.7). Additional information about our treatment of spatial autocorrelation is in Appendix S1.

Model fitting

Models were written in the Bayesian programming language `Stan` (Stan Development Team 2019) and analyzed in the `R` environment (R Core Team 2019; Stan Development Team 2020). Packages used for our analysis are listed in Appendix B. We used weakly informative priors and 4 chains with 2000 iterations each. Model fits were visually evaluated by comparing observed values against posterior predictive draws (Fig. B.2–B.5). Parameter estimates with 90% highest posterior density intervals (HPDI) that did not contain zero (or one, when expressed as odds ratios) were

considered to have important, non-zero effects on the response variable. A common default in Bayesian analyses is to use 90% HPDIs because they are more stable than 95% intervals (Goodrich *et al.* 2020).

Results

Across 151 plots, 5798 trees and shrubs were included in our study and 18 species were considered hosts and 9 as nonhosts (Table B.2). Four commonly symptomatic species accounted for 99.6% of detected infections. Symptoms were primarily found on the two most ubiquitous and abundant species, bay laurel (923 symptomatic/1104 total plants, 83.6%) and tanoak (1153 symptomatic/2189 plants, 52.6%), while there were fewer on coast live oak (36 symptomatic/296 plants, 12.2%) and Shreve oak (28 symptomatic/617 plants, 4.5%). The other 14 host species were rarely symptomatic. Of these species, only 8 redwoods and 1 California buckeye (*Aesculus californica*) were symptomatic.

How density varies with richness

Total basal area of all species remained constant across richness in both forest types (Fig. 2.3A). Bay laurel occurred more frequently in richer plots, while tanoak occurrence did not vary strongly with richness (Fig. 2.3B, 2.3C). When present, the basal area of bay laurel had a weakly negative relationship with richness (median, 90% HPDI = -0.15 [-0.31, 0.03]), whereas that of tanoak did not vary considerably (-0.08 [-0.29, 0.14]; Fig. 2.3B, 2.3C). Additionally, the number of rarely symptomatic host plants increased with richness, while the number of commonly symptomatic host plants did not change substantially (Fig. 2.3D, 2.3E).

How community competence varies with richness

Mixed evergreen and redwood forest communities were both significantly nested (mixed evergreen: $NODF_{obs}$ = 50.2, P < 0.001; redwood: $NODF_{obs}$ = 58.5, P < 0.001), indicating that depauperate communities were nested subsets of their richer counterparts (Fig. 2.4A). Species-poor communities were more likely to contain ubiquitous species, while richer communities also
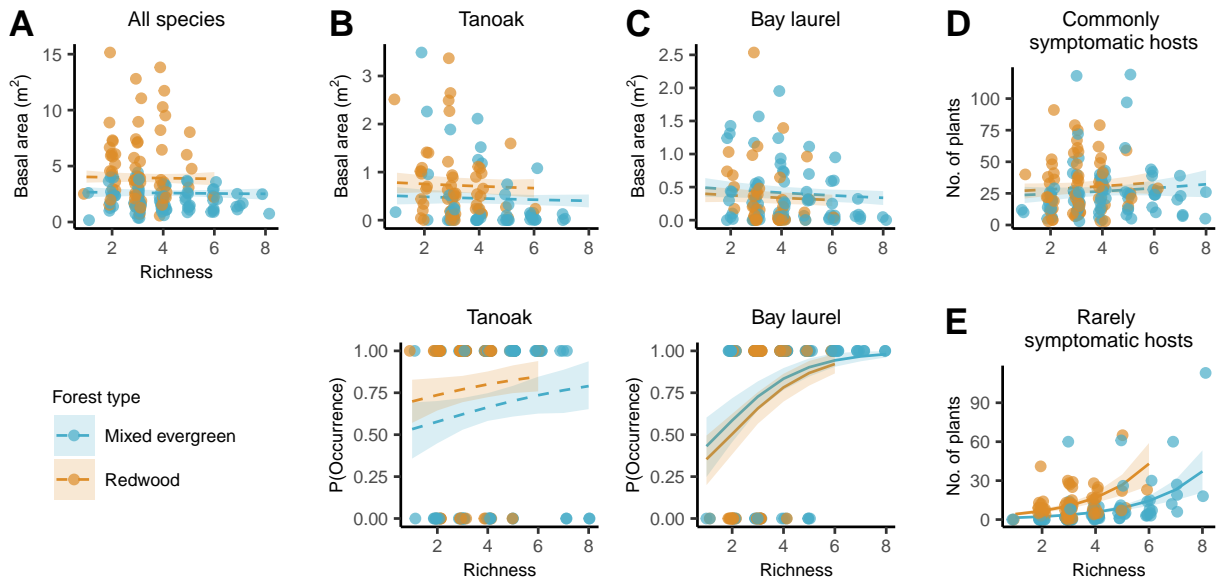
Figure 2.3: Relationships between richness and various measurements of plant density by forest type. A) Density measured as total plant basal area. B, C) Hurdle models measuring tanoak or bay laurel density, which assessed probability of occurrence (bottom) and, conditional upon presence, assessed basal area (top). D) Density measured as number of commonly symptomatic host plants. E) Density measured as number of rarely symptomatic host plants. Points are horizontally jittered. Lines and shaded regions represent the median and 90% HPDI of the posterior estimate of the mean. Solid lines indicate the 90% HPDI of the effect of richness did not cross zero.

consisted of rarer species, which tended to be less competent. Bay laurel and tanoak were more competent than the other measured species (Fig. 2.4B). Within mixed evergreen forests, the species that contributed most to community competence were bay laurel followed by tanoak, and in redwood forests they were tanoak, followed by bay laurel and redwood (Fig. 2.4C). Although redwood is a low-competence host, it is the largest tree species in the forest and very common. Total community competence was higher in redwood forests than mixed evergreen forests and it declined in plots with higher richness (Fig. 2.4D).
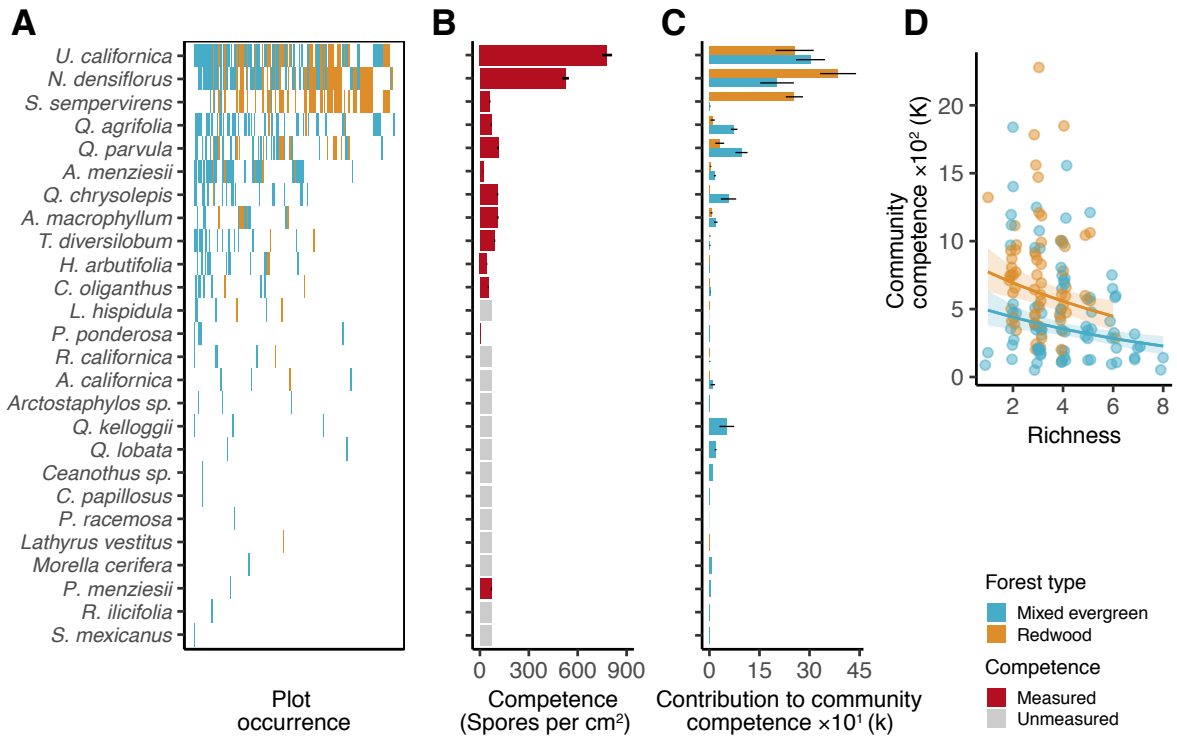
Figure 2.4: Nestedness and the linkages between host competence and diversity in both forest types. A) Matrix of species that are present among the 151 study plots. The top rows represent the most ubiquitous species and the leftmost columns represent the richest plots. In a perfectly nested set of communities, the depauperate communities would consist of a subset of the species present their richer counterparts, causing this matrix to be filled entirely in the upper left-hand side. B) Sporulation potential (mean $\pm$ SE) as assessed in laboratory inoculation assays. Species are in order of rank ubiquity. C) Each species' contribution towards community competence (mean $\pm$ SE). D) The relationship between richness and community competence with points horizontally jittered. Line and shaded region represents the median and 90% HPDI of the posterior estimate of the mean. Solid lines indicate the 90% HPDI of the effect of richness did not cross zero. Species not included in the laboratory sporulation assays (grey) are estimated as the median of those that were measured. Analyses are shown separately for each forest type, mixed evergreen (blue) and redwood (orange).

How disease risk varies with richness, known competent hosts, and community competence

Across all models, surrounding host vegetation had consistently positive effects, redwood forests and historical precipitation levels had negative or no effects, and sampling year and PSI had negligible effects on community- and individual-level disease risk (Table B.3-B.5). After accounting for variation related to these factors, the importance of richness on disease risk and its association with known competent hosts and community competence varied depending on how disease was measured.

Disease prevalence aggregated among all hosts in the community decreased with richness (median odds ratio, 90% HPDI = 0.68 [0.49, 0.90]; Fig. 2.5A). We included bay laurel basal area, tanoak basal area, and community competence into subsequent models, all of which had positive effects (Fig. 2.5A). After accounting for variation in bay laurel and tanoak density, the negative richness-disease covariance weakened only slightly (0.70 [0.52, 0.96]), and it further weakened when community competence was instead incorporated (0.79 [0.58, 1.08]). Disease prevalence was best predicted by the model featuring richness and host basal area (M2), outperforming the models including community competence (M3: ΔELPD $= -13.9$, SE$_\Delta$ $= 3.6$) and richness only (M1: ΔELPD $= -20.1$, SE$_\Delta$ $= 5.8$).

When detected infections were examined exclusively among the four commonly symptomatic species, richness no longer had a nonzero effect on disease prevalence (odds ratio: 0.84 [0.61, 1.17]; Fig. 2.5B). Bay laurel and community competence had positive effects, while the effect of tanoak diminished. The negligible effect of richness did not change when models included host basal area or community competence. The model with richness and host basal area (M2) performed better than the models with community competence (M3: ΔELPD $= -16.8$, SE$_\Delta$ $= 4.7$) and richness alone (M1: ΔELPD $= -23.7$, SE$_\Delta$ $= 6.7$).

Individual-level disease risk models accounted for species-specific disease rates, which were highest for bay laurel, followed by tanoak, coast live oak, and Shreve oak (Fig. 6A). The models also controlled for size-dependent variation in susceptibility, which was greater for larger individuals (Table B.5). Richness on average was not strongly correlated with disease risk in the model including
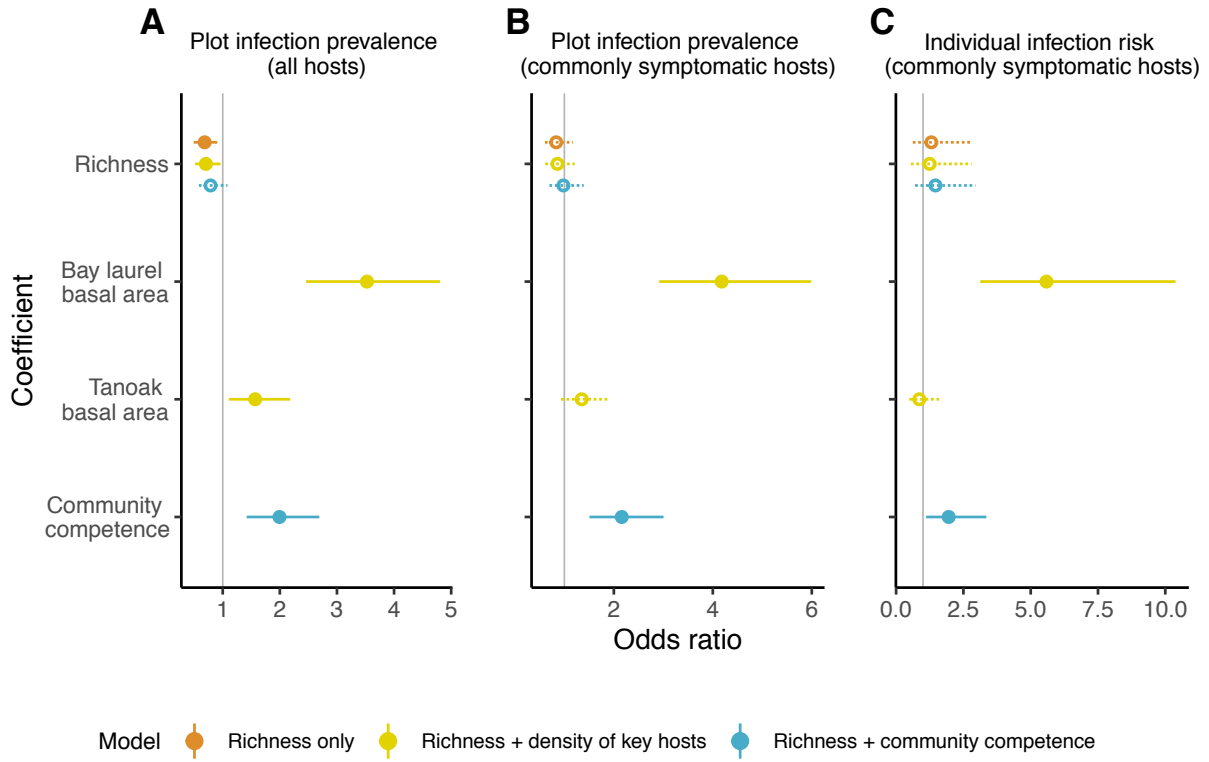
Figure 2.5: Effects of community-related covariates of disease risk models evaluated as A) community-level disease prevalence for all hosts, B) community-level disease prevalence for commonly symptomatic hosts, and C) individual-level disease risk for commonly symptomatic hosts. Note that panel C shows the mean effect of richness (beta_bar, equation 2), while species-specific parameters of the individual-level disease risk models are displayed in Fig. 6. The three colors represent the three explanatory models (M1. Richness only, M2. Richness + density of key hosts, M3. Richness + community competence) being contrasted within each disease risk metric. Posterior estimates are displayed with the median and 90% HDPI, with intervals not crossing one shown with a solid line and closed points.

richness only (odds ratio: 1.31 [0.62, 2.75]), and its effect did not substantially change after including predictors for host basal area or community competence (Fig. 2.5C). Across the three explanatory submodels, species-specific effects of richness for coast live oak, Shreve oak, and tanoak were unlikely important (90% HPDI contained one); meanwhile, richness had a positive effect on disease risk for bay laurel, with credible intervals slightly smaller or larger depending on the covariates included in the model (Fig. 2.6B). Disease risk was not strongly correlated with tanoak basal area, positively correlated with community competence, and strongly, positively correlated with bay laurel basal area (Fig. 2.5C). The model including richness and host basal area (M2) marginally outperformed models including community competence (M3: ΔELPD = -3.7, $SE_\Delta = 2.3$) or richness alone (M1: ΔELPD = -4.9, $SE_\Delta = 2.5$).
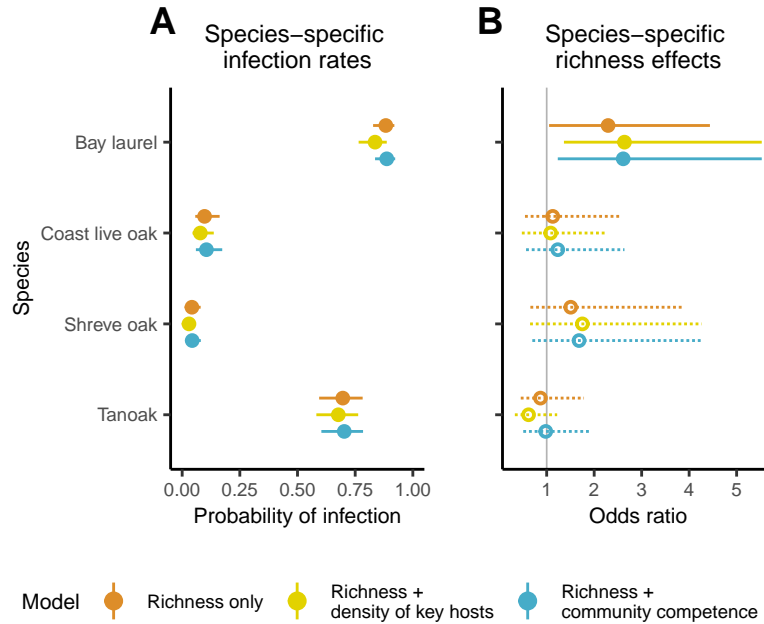
Figure 2.6: Additional posterior estimates of the individual-level disease risk models, including species-specific A) intercepts and B) effects of richness, representing alpha_s and beta_s for species s, respectively (see equation 2). Posterior estimates are displayed with the median and 90% HDPI, with intervals not crossing one shown with a solid line and closed points.

Discussion

Despite frequent tests of negative diversity-disease relationships in natural ecosystems, the mechanisms remain poorly resolved. We tested how relationships among species richness, densities

of keys hosts, community competence, and disease risk metrics vary in a forest system previously shown to exhibit negative diversity-disease patterns (Haas *et al.* 2011). Richness had no limiting effect on individual-level disease risk, and therefore neither competent host regulation nor encounter/transmission reduction were possible dilution mechanisms. Rather than depending on the composition of the entire community, average risk of acquiring disease was largely driven by a single, common, highly competent host, bay laurel (Fig. 2.5C). This species' density did not have a clear relationship with richness, which may explain the lack of a dilution effect evaluated at the individual level. In contrast, the negative effect of richness on community-level disease prevalence was solely attributable to its positive covariance with the number of rarely symptomatic host species. Rarely symptomatic host species reduced the relative density of commonly symptomatic hosts without significantly altering their individual risks of disease (Fig. 2.1C). Aggregating disease prevalence at the community level may misattribute dilution mechanisms and bias toward negative diversity-disease relationships, which has consequential implications for the effects of conserving biodiversity in disease-impacted ecosystems.

Diversity-associated mechanisms of individual-level disease risk

While multiple host species of varying competence may contribute to transmission risk (Hamer *et al.* 2011; Searle *et al.* 2016), sometimes generalist pathogens are influenced by the presence of a single host species (Wilber *et al.* 2020). The risk of acquiring disease symptoms primarily depended upon the basal area of bay laurel, which we uncovered using models that estimated individual-level disease risk. Less competent hosts were not essential in predicting disease risk. Consistent with other field studies in California, basal area of the next most competent host, tanoak, was not influential (Swiecki & Bernhardt 2002; Meentemeyer *et al.* 2008a; Simler-Williamson *et al.* 2021) and community competence, a weighted mean of all species' transmission potentials, had a weaker effect than bay laurel and did not improve model predictive performance relative to the model including bay laurel density. Accordingly, much of the effect of richness hinged upon its correlation with bay laurel occurrence and abundance.

Theory predicts that when the most competent species has a low extirpation risk, communities are nested, and total density remains invariant with diversity ('substitutive assembly'), there should

be a higher density of competent hosts in species-poor communities (Rudolf & Antonovics 2005; Joseph *et al.* 2013; Mihaljevic *et al.* 2014). Each of these conditions was met and indeed, we found that the basal area of bay laurel was slightly higher in depauperate communities (Fig. 2.3A). However, bay laurel was also less likely to persist in species-poor communities (Fig. 2.3A). The combined effect of these two opposing variables (basal area and occurrence) likely led to a weak overall association between bay laurel density and richness, and no corresponding shift in individual-level disease risk averaged among the commonly symptomatic species.

By contrast, community competence, based on laboratory sporulation assays, did decline with richness, and yet this did not lower individual-level disease risk in more diverse plots. Measurements from artificial inoculations do not integrate variation due to host phenology, forest structure, and climate (Dodd *et al.* 2008; Davidson *et al.* 2011; Simler-Williamson *et al.* 2021; Rosenthal *et al.* in press), nor variation within species or individuals (Stewart Merrill & Johnson 2020). These challenges are logistically difficult to overcome for such a broad set of large, long-lived tree species. Community competence currently weights the contribution from bay laurel and less competent hosts. If community competence were calibrated to more accurately reflect natural inoculum pressure, it might primarily reflect bay laurel density.

When effects of richness were parsed for each species, richness had undetectable effects on disease risk for tanoak or oaks, but it had a positive effect for bay laurel. This result could be highly impactful given how central bay laurel is to pathogen spread. The positive effect of richness may reflect a correlation with unaddressed, disease-inducing factors, such as microclimates or pathogen invasion history. Plots with greater richness may have been invaded earlier by this nonnative pathogen, and thus *P. ramorum* would have more time to spread within those stands (Cobb *et al.* 2020).

Diversity-associated mechanisms of community-level disease risk

Richness was negatively associated with disease prevalence for all hosts in a plot, which is best explained by the relative abundance of commonly symptomatic species. The number of rarely symptomatic host plants increased with richness, while the number of commonly symptomatic plants (accounting for 99.6% of detected infections) did not change. The proportion of commonly

symptomatic hosts negatively covaried with richness, limiting the fraction of community-wide disease. Without rarely symptomatic species, models of community-level disease prevalence led to similar conclusions as the individual-level analysis—bay laurel density drove detected infections and richness did not have a strong effect. By aggregating disease among all hosts in a community, low-competence, rarely symptomatic hosts numerically diluted the proportion of symptomatic plants without affecting transmission risk to susceptible populations.

Differences in the diversity-disease relationship across hierarchical levels

Individual- and community-level disease risk varied independently with respect to the density of competent hosts and proportion of symptomatic hosts, respectively. Thus, the direction and drivers of the diversity-disease relationship are distinct across hierarchical levels. However, this distinction is easily conflated. For instance, the negative effect of richness on community-level disease prevalence remained after accounting for tanoak and bay laurel densities. Haas *et al.* (2011) acquired similar results and hypothesized richer communities contained either more noncompetent plants that interfered with inoculum dispersal pathways ('encounter reduction'; Fig. 2.1B), or fewer asymptomatic, competent hosts that illusively caused infections ('competent host regulation'; Fig. 2.1A). Noncompetent species inhibit encounter rates when they can physically block local transmission. Pathogens with root-to-root transmission are good candidates to observe this mechanism, unlike *P. ramorum* where sporangia travel distances of up to 4 km (Hansen *et al.* 2008; Mascheretti *et al.* 2008). Yet, richness became unimportant after adding community competence to the model predicting community-level prevalence (Fig. 2.5A), suggesting that asymptomatic transmission from many forest species may explain the negative diversity-disease relationship. However, we instead interpret this finding as a spurious correlation since our individual-level models indicate that bay laurel was the primary host driving disease.

Community-level observations cannot directly explain processes occurring between (susceptible and infectious) individuals, and our study represents a case of Simpson's paradox, in which correlations are not preserved during data aggregation (Simpson 1951). Salkeld & Antolin (2020) illustrated that disease aggregated across large spatial scales can lead to spurious correlations with diversity and explanatory factors, and these relationships might reverse if reexamined using

individual- or species-level data. Our results, and others' (Piudo *et al.* 2011), confirm that aggregating disease at the community level can generate this pattern. Although not examined in our study, community-wide disease caused by multiple pathogens (e.g. "community pathogen load" *sensu* Mitchell *et al.* 2002, which also averages across species) can produce similar mismatches (e.g. Hantsch *et al.* 2013). To be clear, we believe individual- and community-level disease metrics are equally valid and important to study; however, mechanisms used to explain diversity-disease relationships need to reflect the levels at which disease was measured.

We also suspect that community-level prevalence may negatively correlate with diversity more frequently than individual-level disease risk under specific assembly patterns. When depauperate communities are dominated by disease-prone species—which is more often the case than not (Joseph *et al.* 2013; Gibb *et al.* 2020), even in the absence of dilution mechanisms, less susceptible species added to higher diversity communities would increase the likelihood of observing a decline in overall prevalence. Diversity often negatively covaries with community-level prevalence (Bradley *et al.* 2008; Moore & Borer 2012; Liu *et al.* 2018), but not always (Vaz *et al.* 2007; Hydeman *et al.* 2017; Milholland *et al.* 2017). Community-wide disease risk is not uncommon under the dilution effect purview (Table B.1), and whether it biases toward negative diversity-disease relationships deserves closer attention.

Given that diversity-disease relationships may change across hierarchical levels, what was the most appropriate measure of disease? Response variables need to match questions meaningful to management (Johnson *et al.* 2015a). Managing for ecosystem health is an important goal. In our system, the overall percentage of diseased host plants is critical for predicting how disease-induced mortality affects fuels, carbon sequestration, or resilience to large-scale disturbance (Metz *et al.* 2011; Simler *et al.* 2018; Cobb *et al.* 2020). Conserving biodiversity may still improve ecosystem health when richness is correlated with a lower proportion of susceptible species. Other times, the goal is to manage the health of specific hosts, which aligns with the majoritarian notion of the dilution effect. We examined disease risk in four species and accounted for differences in species-specific susceptibility. Here, maintaining diverse forest stands would not reduce the risk of individuals acquiring disease and targeted management of bay laurel is needed.

Conclusion

Two unresolved topics in disease ecology involve exploring how diversity correlates with species composition and the consequences on disease risk, and how disease measured at the individual or community level affects conclusions (Johnson *et al.* 2015a). We found that the overall density of the most competent species likely did not have a strong relationship with richness and, consequently, richness did not limit individual-level disease risk. Empirical tests of this pattern must continue in other naturally assembled communities, especially in forests and other understudied systems. We also found that richness can have a positive or negligible effect on disease at the individual level while concomitantly having a negative effect at the community level. Understanding these multilevel differences is key for managing the health of the ecosystem versus specific forest species. Looking forward, one solution is to explicitly define the currently vague description of 'disease risk', which will require discussion among research, management, and policy priorities (see Keesing *et al.* 2006). A more expansive prospect is for researchers to contrast various metrics of disease to uncover how, why, and for which species biodiversity affects disease.

Chapter 3. Species densities, assembly order, and competence jointly determine the diversity-disease relationship

Lisa M. Rosenthal[1,2], Wesley R. Brooks[3], David M. Rizzo[2]

[1] Graduate Group in Ecology, University of California, Davis, CA 95616, USA

[2] Department of Plant Pathology, University of California, Davis, CA 95616, USA

[3] DataLab, University of California, Davis, CA 95616, USA

Abstract

Since individual species vary in abundance and host competence, variation in species composition strongly influences disease dynamics. Forecasting effects of species composition on disease depends on community (dis)assembly, the processes determining how species are added (or lost) from communities. We simulated community assembly by planting mesocosms, nested along a richness gradient, and tested how relationships between richness and either species loss order or overall density affect disease risk. Mesocosms containing up to 6 crop species of varying competence were inoculated with a soilborne fungal pathogen, *Rhizoctonia solani*. Disease was measured as species-level prevalence, community-level prevalence, and total number of diseased plants. Regardless of metric, richness limited disease when species loss order negatively correlated with competence and overall species density was intransient with richness. When total density increased with richness or species were lost randomly, richness primarily correlated positively or weakly with disease. Our results are consistent with theoretical expectations and represent the first empirical study simultaneously testing the influence of species densities, disassembly order, and competence on diversity-disease relationships.

Introduction

How does community assembly affect disease risk? Since host species vary in their ability to become infected and transmit a given pathogen (i.e. 'host competence'), patterns in community (dis)assembly, defined as processes that determine which species and how many are added (or lost)

from communities, can differentially impact infectious disease in communities undergoing biodiversity loss (Joseph *et al.* 2013; Halliday *et al.* 2019). Understanding how and when species loss influences disease dynamics is paramount for predicting and managing future outbreaks; addressing the role of community assembly may be key for identifying conditions underlying diversity-disease relationship in natural ecosystems.

When highly competent host species are least likely to be extirpated during species loss, there is an increased likelihood that diversity and overall transmission risk negatively covary (Ostfeld & LoGiudice 2003), a phenomenon termed the 'dilution effect' (Keesing *et al.* 2006). Negative relationships between competence and extirpation risk may be attributed to life history tradeoffs. For example, 'weedy' species tend to dedicate fewer resources to disease resistance (Cronin *et al.* 2010; Heckman *et al.* 2019). However, deterministic and stochastic forces shape community disassembly (Fukami *et al.* 2005; Halliday *et al.* 2019). When species loss order is unrelated to host competence, changes in disease risk are less predictable and the diversity-disease relationship is expected to be idiosyncratic (Ostfeld & LoGiudice 2003; Joseph *et al.* 2013).

Even when competence negatively correlates with extirpation risk, changes in disease also depend on how overall density covaries with diversity loss (Searle *et al.* 2016). At one extreme, total community abundance may remain invariant with richness. Under this 'substitutive assembly', a loss of diversity may release competent host species from strong resource limitations, leading to a higher absolute density of competent hosts, and therefore, higher disease risk in species-poor communities (Rudolf & Antonovics 2005; Mihaljevic *et al.* 2014). Conversely, community abundance may positively correlate with diversity ('additive assembly'), such that the densities of individual species do not covary with richness. Host densities would be greatest in species-rich communities and for generalist pathogens with density-dependent transmission, disease risk should positively correlate with diversity (Rudolf & Antonovics 2005; Mihaljevic *et al.* 2014). Altogether, it is expected that a negative diversity-disease relationship is most likely when community assembly is substitutive and extirpation risk negatively correlates with competence (Joseph *et al.* 2013; Johnson *et al.* 2015a).

Despite a strong theoretical foundation explaining how competence, species order loss, and abundance may influence the diversity-disease relationship, empirical tests are limited. Correla-

tional studies of natural communities are powerful for identifying how species composition varies across richness levels (Johnson *et al.* 2013; Lacroix *et al.* 2014), which is essential for predicting how communities would likely disassemble. Nevertheless, the effects of different assembly patterns on disease risk may be best addressed under an experimental framework where species composition can be manipulated independently of diversity. To date, experimental studies focused on the dilution effect have compared random versus non-random species loss (Liu *et al.* 2018; Johnson *et al.* 2019) and additive versus substitutive assembly (Johnson *et al.* 2013; Wojdak *et al.* 2014). However, interactions between these two influential axes of community assembly have yet to be empirically investigated.

Moreover, the relationship between diversity and disease can be sensitive to whether disease is measured at the community or species level. The dilution effect typically addresses how diversity impacts the risk of individuals acquiring disease, and hence disease is evaluated for particular host species. The dilution effect has also been assessed using community-level disease metrics, including total propagule load (e.g. Young *et al.* 2014) or average community disease severity or prevalence (e.g. Haas *et al.* 2011; Mitchell *et al.* 2002), which capture overall transmission potential or disease burden, respectively. Despite their fundamental epidemiological differences, various metrics of disease for focal species and overall host communities frequently appear together in the dilution effect literature and can lead to divergent outcomes on diversity-disease patterns (Rosenthal *et al.* in press).

Here we used artificial plant mesocosms to examine the effects of species identities and densities on disease caused by a fungal plant pathogen, *Rhizoctonia solani.* This generalist soil-borne pathogen causes visible aboveground damping-off symptoms when it infects belowground host tissue (Otten *et al.* 2003). Transmission occurs between plants through infective hyphae and slows or arrests when resources are unavailable (Bailey *et al.* 2000). Mesocosms inoculated with *R. solani* are ideal for testing community disease ecology theory because symptoms are obvious, epidemics are fast, high replication is feasible, and environmental conditions, host heterogeneity, and inoculum amounts are relatively easy to control (e.g. Otten *et al.* 2001, 2003, 2005).

We planted mesocosms spanning a plant species richness gradient to test how communities with random and non-random species loss order, as well as communities with substitutive and

additive assembly, affect disease risk. We measured disease at the community and species level to explore how disease metrics might affect conclusions. To explain variation in disease risk under different assembly patterns, we assessed the direct effects of richness, species identities, and densities on species-level disease prevalence. Our study empirically investigates how community assembly affects the diversity-disease relationship, which is important for understanding of how biodiversity loss may impact emerging diseases.

Methods

Study system

We used a model system to test how species composition affects disease risk in a greenhouse experiment. Mesocosm communities were planted and select individuals were inoculated with *R. solani* (AG2-1, Genbank accession #MZ496522). Generalist pathogens are frequently transmitted via a small subset of hosts, despite being able to infect a larger consortium of hosts. We mimicked this pattern by choosing 6 commercially available crop plants that vary in competence. To estimate competence, we summarized intra-specific plant-plant transmission (rather than inoculum-plant transmission) by measuring disease prevalence of all uninoculated individuals (more details below). Host plants included radish (high competence), arugula (moderate), and basil, red romaine, green lettuce, and butter lettuce (low). These plants were also selected because they germinate at high rates and emerge at similar times.

Experimental design

We simulated community disassembly by creating series of mesocosm communities with 1, 2, 4, and 6 crop species (Fig. C.1, Fig. C.2). To be consistent with typical ecological communities, depauperate assemblages contained a nested subset of their richer counterparts (Stephens *et al.* 2016) and relative species abundances followed a log-normal distribution (Roche *et al.* 2012). Within each series, the density (total number of individuals) was either positively correlated with richness ('additive assembly') or remained constant ('substitutive'). Communities with substitutive assembly contained 238 individuals and those with additive assembly consisted of 85, 154, 238,

and 304 individuals. Additionally, the relationship between host competence and the order in which species were lost was either strongly positive ('non-random assembly order') or idiosyncratic ('random'). For example, the non-random disassembly treatment consisted of the same species order for each replicate—that is, high-competence radish was always present and most abundant, while low-competence butter lettuce was rarest. Meanwhile, the random order treatment had a different disassembly order for each replicated series. Using a 2x2 factorial design, we manipulated two axes of community disassembly across a richness gradient to test how patterns in species loss affect disease risk (4 richness levels x 10 replicated series = 40 mesocosms for each treatment).

Additional mesocosms were created for various reasons. To estimate host competence, we ensured that for each species, there were at least 4—6 single-species communities consisting of 238 individuals. To estimate background damping off symptoms and germination rates, we planted one single-species mesocosm for each species at the highest density of 304 individuals. These controls were not inoculated. Our analysis of disease risk also parses effects of richness from densities of species and with the design as described above, the relative abundance of radish negatively correlates with richness. To better decouple the two variables, we augmented the design with nine trays that had higher relative densities of radish (Fig. C.3).

Pathogen inoculations and disease assessment

Mesocosms were planted in seedling propagation trays (25.4 x 25.4 x 6.2 cm) filled with auto-claved sand with 10% by weight fertilizer mix (in-house formula for plant growth). Over the course of three days (trays split randomly), seeds were directly sown in a hexagonal grid, dusted with 150 ml of vermiculite, and covered with a clear humidity dome. Locations of seeds were randomly assigned (Fig. C.2) and trays were randomized within the greenhouse. Trays were watered every 2–3 days and weighed to ensure consistent application. Plants grew under 16 h artificial light and air temperature was 23°C on average. Soil temperature nonetheless varied and on the last day, was measured in all trays with a thermometer probe.

On day three, once the majority of seedlings emerged, 12 individuals per tray were inoculated with *R. solani*. Species of challenged plants were selected proportionally to their relative abundances. Inoculum was prepared by scattering double-autoclaved poppy seeds onto 4-day-old fungal

colonies grown on potato dextrose agar, and incubating at 24°C in the dark for three additional days (Otten et al. 2001). Colonized poppy seeds were individually placed under soil line 2 mm away from challenged plants. Plants were considered diseased when they exhibited aboveground symptoms, which include basal stem lesions and/or seedling collapse. On day 18, the final disease statuses of individuals were recorded. Non-emerged plants, plants killed by herbivores, and one tray that was accidently not watered were omitted from analysis.

At the end of a preliminary trial, seedlings with and without disease symptoms (10 each for all species) were plated onto Rhizoctonia solani-selective media (water agar supplemented with chloramphenicol and benomyl; Paulitz & Schroeder 2005). Seedling crowns were surface sterilized (5% bleach 30 s, rinsed with water), plated, and visually inspected for hyphae at 24 and 48 h. All symptomatic plants produced hyphae after 24 h, confirming that disease symptoms were good proxies for *R. solani* infections. Some asymptomatic plants of radish (40%), basil (30%), arugula (10%), and green romaine (10%) produced hyphae after 48 h. Although potentially less virulent, latent or pre-symptomatic infections are possible in this study system.

Statistical analyses

Diversity-disease relationships as a function of community disassembly

To understand how the diversity-disease relationship may change under different disassembly patterns, we analyzed communities undergoing four assembly treatments: i) additive, non-random; ii) substitutive, non-random; iii) additive, random; and iv) substitutive, random. Using separate generalized linear (mixed) models (GL(M)M) for the four treatments, we analyzed disease at the community and species level to determine how disease metrics may alter conclusions.

At the community level, disease of non-challenged plants was estimated as total disease prevalence using a beta-binomial likelihood and number of diseased plants using a negative binomial likelihood. Models included an effect for richness and controlled for day planted and soil temperature. At the species level, disease prevalence of non-challenged plants was estimated for each host species using a beta-binomial likelihood. Models controlled for day planted and temperature and included species-varying intercepts and coefficients of richness and a tray-varying intercept. Green

lettuce and butter lettuce were omitted from analysis of the deterministic treatments since they were only present in the highest richness level. Extra single species trays were included in the analysis of the substitutive, random treatment since they would only improve model certainty and not bias the results.

Drivers of species-level disease prevalence

To explore drivers of variation in disease risk, we assessed effects of richness and species densities on species-level disease prevalence. Here, we evaluated disease from all mesocosm trays together (rather than the four treatments separately). With a beta-binomial likelihood, disease prevalence was estimated by modeling the number of diseased plants of each species in each tray, given the total number of non-challenged plants. Models included species-varying intercepts and coefficients of richness, terms to control for day planted and temperature, and a tray-varying intercept. We contrasted models with additional tray-level covariates, which included combinations of individual species densities and total density of all other species. Densities of individual species were square root transformed to spread the right-skewed distribution and all variables were centered and scaled by dividing by 2 SD (Gelman 2008). Predictive performance of models were compared based on the difference in expected log pointwise predictive density (ELPD) using 10-fold cross-validation (Vehtari *et al.* 2017).

Model fitting—GL(M)Ms were coded in R (R Core Team 2019) and estimated using Bayesian methods from the package `brms` (Bürkner 2017). We used weakly informative priors and 4 chains with 2000 iterations each. Model fits were visually evaluated by comparing observed values against posterior predictive draws and for convergence, we ensured Rhat values were ≤ 1.01 (Vehtari *et al.* 2020). Parameter estimates with 90% highest posterior density intervals (HPDI) that did not contain zero were considered to have important, non-zero effects.

Results

A total of 36,922 seedlings in 171 mesocosms were monitored and analyzed for symptoms. Also 1,824 seedlings were grown in 6 single-species uninoculated trays. Germination rates were 95–100% and background disease symptoms were nonexistent. Host competence was estimated as disease

prevalence in monospecific trays for the following species: radish (mean, SD = 0.94 [0.08]), arugula (0.33 [0.27]), basil (0.03 [0.02]), red romaine (0.02 [0.02]), green lettuce (0.006 [0.005]), and butter lettuce (0.02 [0.006]).

Diversity-disease relationships as a function of community disassembly

With additive assembly, community disease prevalence positively correlated with richness, regardless of whether species loss order was non-random or random (Fig. 3.1a, 3.1c). With substitutive assembly and random species loss, richness likely had an unimportant association (Fig. 3.1d). Only with substitutive and non-random disassembly did richness have a strongly negative effect on community disease prevalence (Fig. 3.1b). Results were qualitatively identical for density of diseased plants (Fig. C.4).

Figure 3.1: Relationships between richness and community-level disease prevalence for different community assembly patterns. Lines and shaded regions represent the median and 90% HPDI of the posterior estimate of the mean. Solid lines indicate the 90% HPDI of the coefficient of richness did not contain zero.

When disease prevalence was evaluated for particular host species, effects of richness were strongly positive with additive assembly (Fig. 3.2a, 3.2c). For communities with substitutive, non-random disassembly, the 90% HPDI of the coefficient for richness was entirely negative for all

species, except red romaine where the interval was [-1.87, 0.09] (Fig. 3.2b). For communities with substitutive, random disassembly, the effects of richness were negative for radish, positive for green lettuce, and negligible for all other species (Fig. 3.2d).
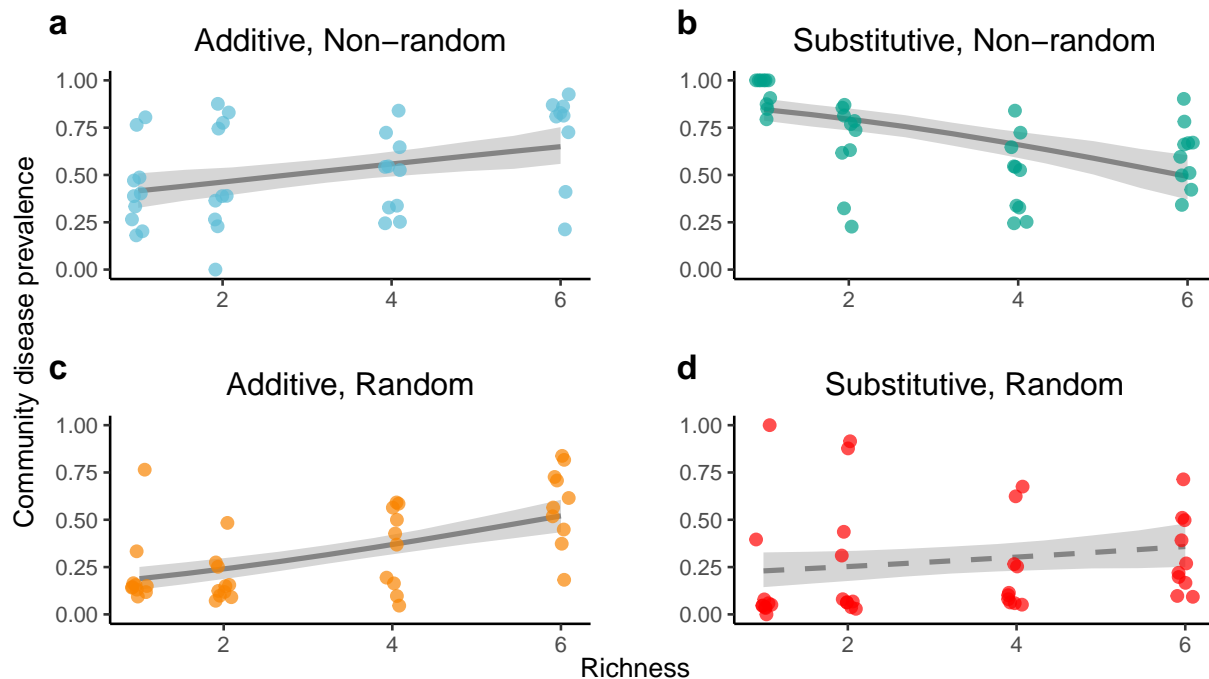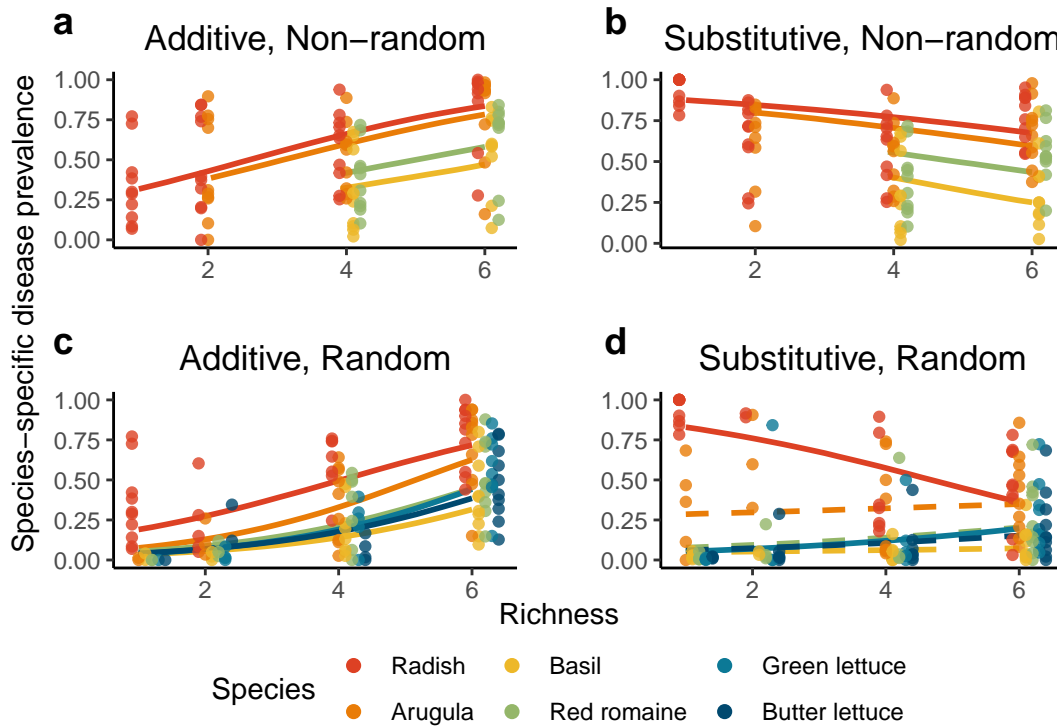

Figure 3.2: Relationships between richness and species-level disease prevalence for different community assembly patterns. Solid lines indicate the 90% HPDI of the coefficient of richness did not contain zero.

Drivers of species-level disease prevalence

After controlling for soil temperature, which had a negative effect, and planting day, the importance of richness on species-level disease prevalence varied depending on which other tray-level variables were accounted for (Table C.1). Richness positively covaried with disease risk in the model incorporating total density, which also had a strong positive effect. Yet, the importance of richness weakened when information on the densities of specific species was included. In the model including densities of each species, the mean coefficient of richness was likely unimportant (median log-odds, 90% HPDI =0.46 [-0.19, 1.17]), densities of radish (3.63 [2.94, 4.45]) and arugula (0.85 [0.29, 1.4]) had strongly positive effects, while densities of other species had weak effects. As long

as radish density was explicitly modeled and densities of other species were included (see Table C.1 for details), predictive performance was equivalent and superior to the model incorporating total density only (ΔELPD, SE = -52.2, 10.6).

Discussion

Theory predicts that whether species loss enhances or suppresses disease risk depends on community assembly (Joseph *et al.* 2013). We empirically contrasted the relationship between richness and various disease metrics in communities with different assembly patterns. Whether disease was measured for focal species or the overall host community, our results closely aligned with expectations. Richness limited disease when species loss order negatively correlated with competence ('non-random disassembly') and overall species density remained invariant with richness ('substitutive'). In communities with additive assembly or those with substitutive and random disassembly, richness was positively or weakly associated with disease, apart from a few deviations. The effect of richness on species-level disease prevalence was best explained by variation in densities and identities of species, highlighting the consequential impact of compositional shifts on future outbreaks.

In communities with substitutive, non-random assembly, species-level disease risk was likely lower in richer communities because there were fewer competent host plants, such as radish and arugula. 'Competent host regulation' (modified *sensu* Keesing *et al.* 2006), which suggests that a lower density of competent hosts leads to lower transmission risk, is often evoked as a mechanism underlying dilution effects (Johnson *et al.* 2012; Strauss *et al.* 2015). Species-level disease prevalence across all trays was positively associated with richness when density of all species was incorporated into the model; however, the marginal effect of richness was negligible after also conditioning upon the densities of individual species (Table C.1). Densities and identities of species are key for explaining variation in disease risk, and at least in our case, can primarily account for strong richness effects.

For communities with substitutive, random assembly, correlations between richness and species-level disease risk were weak for most species, which is consistent with simulation models measuring overall transmission risk (Joseph *et al.* 2013). Somewhat unexpectedly, radish disease prevalence increased with species loss. The dilution effect for radish is attributed to its strong positive effect

on disease (*c.a.* 16 times stronger than arugula) and to its density negatively covarying with richness. Although densities of host species had an overall random association with richness, for trays containing a given species, density of that species underwent compensatory declines with increasing richness. For example, when radish was present in species-poor assemblages, its density was high and in species-rich assemblages, its density was low. This is an outcome of community nestedness and substitutive assembly. We speculate that irrespective of how competence relates to extirpation risk, strong community nestedness and substitutive assembly can increase the odds of a dilution effect for high competence hosts.

Regardless of species loss order, additive assembly produced positive correlations between richness and species-level disease. Since densities of highly important hosts, radish and arugula, did not increase during disassembly and species-poor communities always contained fewer individuals, depauperate communities fostered less disease. While disease severity on individuals can still be lowest in high-diversity communities despite additive assembly (Johnson *et al.* 2013), this likely represent a special case in which transmission is heavily reduced by direct interactions with non-hosts. We did not detect disease-limiting effects from richness per se and thus, our findings are consistent with simulation models that assume transmission is unaffected by species interactions (Rudolf & Antonovics 2005; Mihaljevic *et al.* 2014).

Diversity-disease relationships were largely insensitive to whether disease was measured at the species or community level (recorded as absolute or relative density of diseased plants). Our findings from substitutive communities—that non-random species loss increased community-wide disease risk and random species loss had little effect—were consistent with experimental studies measuring total infectious propagules (Johnson *et al.* 2019) or community-averaged disease severity (Liu *et al.* 2018). Results from communities with additive assembly, which led to positive associations between disease and richness, further suggest that species loss order has minimal effects on community-level disease when densities of individual species are maintained.

What do results from our experiment, which tested hypothetical endpoints of community disassembly, portend for natural communities? Substitutive and additive assembly might arise when species niches either perfectly overlap or partition, respectively, but a saturating relationship between richness and density may be more realistic. Saturating host abundance should lead to disease

risk rising, then falling across a richness gradient (Mihaljevic et al. 2014). Despite its strong influence on disease dynamics, few studies have examined the relationship between overall host density and diversity in natural ecosystems (but see Guo *et al.* 2006; Rosenthal *et al.* in press) and remains an important topic. Likewise, the strength of the competence-extirpation risk relationship can transform a negative diversity-disease relationship to one that is idiosyncratic. Although disease-prone species tend to be more resistant to perturbations (Gibb *et al.* 2020), extirpations are subject to environmental and demographic stochasticity. Additional stochasticity may weaken any negative extirpation risk-competence associations, add noise to community nestedness, and introduce more uncertainty in diversity-disease patterns. Finally, although various disease metrics did not lead to qualitatively different associations with richness, it is critical to consider what epidemiological information can be gleaned from each metric and its applications to disease management goals.

Overall, our experimental study confirmed many theoretical predictions outlining effects of community assembly on disease risk. It is necessary to continue gathering information on how natural communities will likely (dis)assemble, which involves examining relationships among diversity, species densities, host competence and susceptibility, and likelihoods of extirpation. Through a combination of models, manipulative experimental systems, and surveys of natural communities, we can advance our understanding of how community assembly will impact disease, identify which species loss patterns are most likely to occur under various disturbances pressures, and devise actionable plans to mitigate emerging outbreaks.

Acknowledgements

Appendix

A. Supplementary material, Ch. 1

Table A.1: Results from generalized linear (mixed) models for relationship between spores and species. A total of four separate models were run: two for either spore type (sporangia and chlamydospores) and two for both assays, a) leaf disc and b) leaf dip assay. Since chlamydospores were modeled with a zero-inflated mixture model, parameters predict the probability that the spore counts are from a zero-inflation process, as well as from a negative binomial process.

	Sporangia				Chlamydospores			
	Median	*SD*	*5% CI*	*95% CI*	*Median*	*SD*	*5% CI*	*95% CI*
a) Leaf disc assay								
Inoculum only	-2.59	0.698	-3.69	-1.44	–	–	–	–
ACMA	0.0744	0.228	-0.298	0.45	7.35	0.206	7.01	7.68
ARME	-1.45	0.278	-1.91	-0.997	4.07	0.222	3.72	4.43
CEOL	-0.699	0.243	-1.11	-0.31	7.2	0.207	6.86	7.54
HEAR	-0.857	0.249	-1.27	-0.448	–	–	–	–
LIDE	1.64	0.213	1.28	1.98	2.84	0.454	2.11	3.58
QUAG	-0.398	0.233	-0.793	-0.0313	–	–	–	–
QUCH	0.0547	0.232	-0.342	0.418	–	–	–	–
QUPA	0.0848	0.224	-0.293	0.446	–	–	–	–
TODI	-0.125	0.228	-0.483	0.262	5.46	0.311	4.95	5.98
UMCA	2.03	0.214	1.66	2.36	–	–	–	–
Individual-level intercept variation	1.16	0.0612	1.06	1.26	–	–	–	–
Zero-inflated species ACMA	–	–	–	–	-3.82	1.37	-6.12	-2.19
Zero-inflated species ARME	–	–	–	–	-2.04	0.697	-3.19	-1.07
Zero-inflated species CEOL	–	–	–	–	-3.85	1.29	-5.94	-2.04
Zero-inflated species LIDE	–	–	–	–	1.11	0.439	0.37	1.79
Zero-inflated species TODI	–	–	–	–	0.327	0.344	-0.23	0.892
Phi (dispersion parameter)	–	–	–	–	0.792	0.108	0.625	0.979
b) Leaf dip assay								
LIDE-D	0.945	0.469	0.139	1.68	0.821	0.668	-0.22	1.96
PIPO	-3.13	0.652	-4.14	-2.01	–	–	–	–
PSME	-0.371	0.318	-0.885	0.157	4.19	0.344	3.61	4.72
SESE	-0.517	0.288	-0.973	-0.0223	–	–	–	–
UMCA-D	0.47	0.525	-0.411	1.28	–	–	–	–
Individual-level intercept variation	1.47	0.166	1.21	1.74	–	–	–	–
Zero-inflated intercept	–	–	–	–	0.0968	0.428	-0.55	0.712
Phi (dispersion parameter)	–	–	–	–	0.806	0.375	0.255	1.42

Table A.2: Pairwise contrasts between species intercepts in the sporangia models for a) leaf disc and b) leaf dip assays. Values are the median of 'row − column' differences between the log-posterior values. Larger absolute values indicate larger differences in posterior estimates and bold indicates significance (90th HPDI does not cross zero).

a) Leaf disc assay

	ACMA	ARME	CEOL	HEAR	LIDE	QUAG	QUCH	QUPA	TODI	UMCA
CONTROL	**-2.66**	-1.14	**-1.89**	**-1.74**	**-4.22**	**-2.21**	**-2.65**	**-2.68**	**-2.46**	**-4.61**
ACMA		**1.53**	**0.773**	**0.933**	**-1.56**	0.46	0.01	-0.013	0.206	**-1.95**
ARME			-0.754	-0.594	**-3.08**	**-1.07**	**-1.51**	**-1.54**	**-1.32**	**-3.47**
CEOL				0.163	**-2.32**	-0.304	**-0.761**	**-0.784**	**-0.564**	**-2.72**
HEAR					**-2.48**	-0.474	**-0.928**	**-0.95**	**-0.728**	**-2.88**
LIDE						**2.01**	**1.57**	**1.54**	**1.75**	-0.4
QUAG							-0.45	-0.469	-0.256	**-2.41**
QUCH								-0.0215	0.191	**-1.96**
QUPA									0.217	**-1.94**
TODI										**-2.16**

b) Leaf dip assay

	PIPO	PSME	SESE	UMCAD
LIDED	**4.07**	**1.31**	**1.46**	0.439
PIPO		**-2.77**	**-2.62**	**-3.63**
PSME			0.155	-0.845
SESE				**-1.01**

Table A.3: Results of generalized linear mixed models for relationships between a) sporangia vs. lesion area and b) chlamydospores vs. lesion area.

	Median	SD	5% CI	95% CI
a) sporangia production and lesion area				
Intercept	-0.514	0.495	-1.28	0.335
Lesion area	1.3	0.667	0.223	2.39
Assay	0.255	0.429	-0.469	0.929
Species-level intercept variation	1.39	0.349	0.874	1.96
Species-level slope variation	1.7	0.797	0.402	2.97
Individual-level variation	1.18	0.0605	1.09	1.29
b) Chlamydospore production and lesion area				
Intercept	3.21	0.886	1.76	4.63
Lesion area	2.06	0.978	0.468	3.68
Assay	0.145	0.48	-0.648	0.936
Species-level intercept variation	1.94	0.604	1.13	2.92
Species-level slope variation	1.91	1.05	0.00236	3.3
Zero-inflated intercept	-1.22	0.25	-1.63	-0.807
Zero-inflated species ARME	-0.432	0.364	-1.03	0.156
Zero-inflated species CEOL	-0.864	0.387	-1.5	-0.235
Zero-inflated species LIDE	1.45	0.342	0.858	2
Zero-inflated species LIDE-D	0.06	0.483	-0.758	0.83
Zero-inflated species PSME	0.973	0.348	0.436	1.57
Zero-inflated species TODI	0.702	0.45	-0.0483	1.41
Phi (dispersion parameter)	0.873	0.131	0.652	1.08

B. Supplementary material, Ch. 2
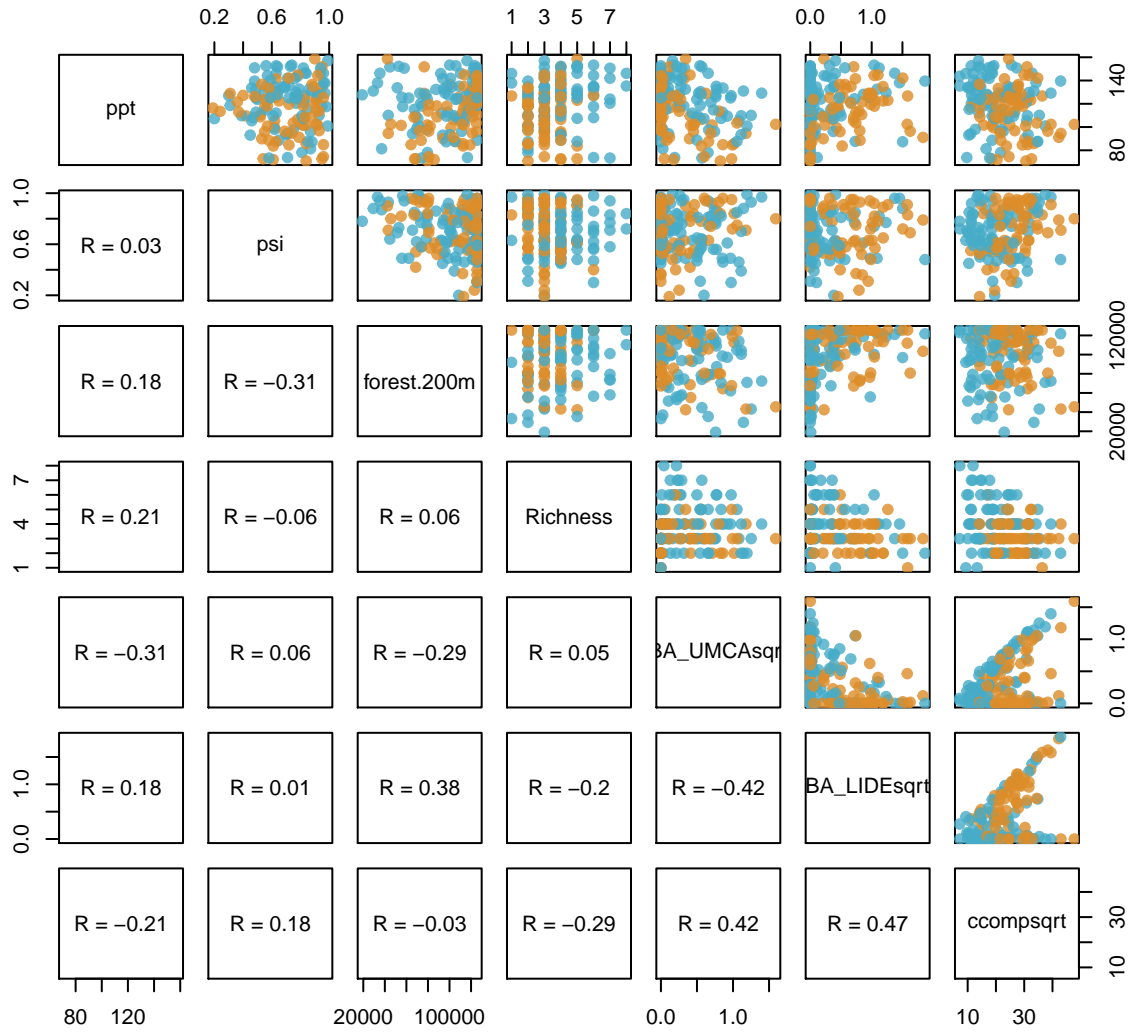
Supplementary figures

Figure B.1: Pairs plots and Pearson's correlations of continuous variables used in the three disease risk model submodels. Orange and blue points designate data from redwood and mixed evergreen forests, respectively.
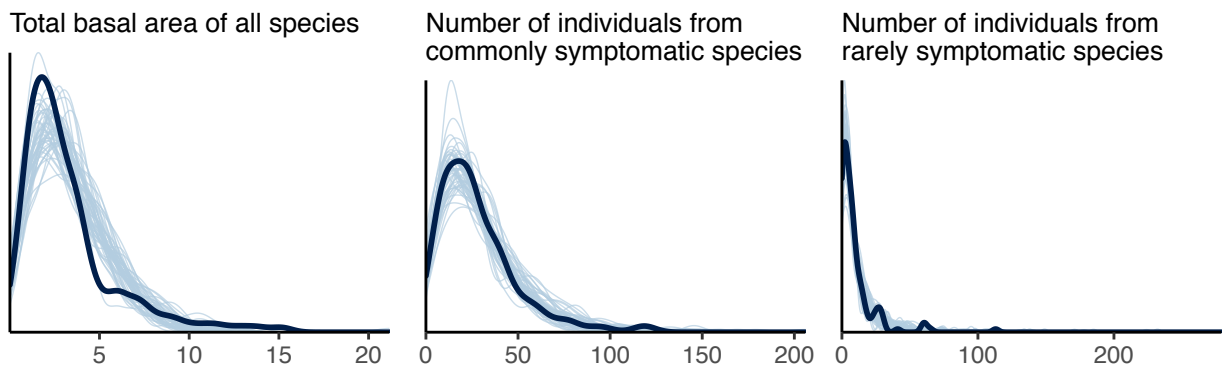
Figure B.2: Density plots of posterior predictions (100 samples, light blue) against observed (dark blue) densities measured as either basal area or number of individual plants.
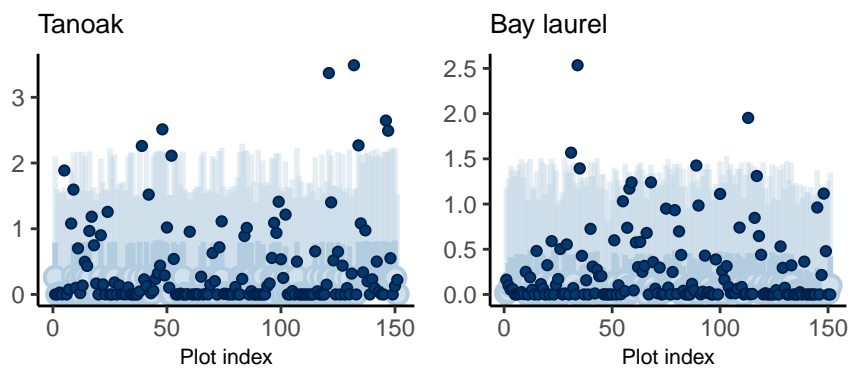

Figure B.3: Intervals of posterior predictions plotted against observed basal areas (dark blue point) in each plot of the top 6 most commonly occurring species. The 50% (medium blue) and 90% (lightest blue) of the probability mass are shown.
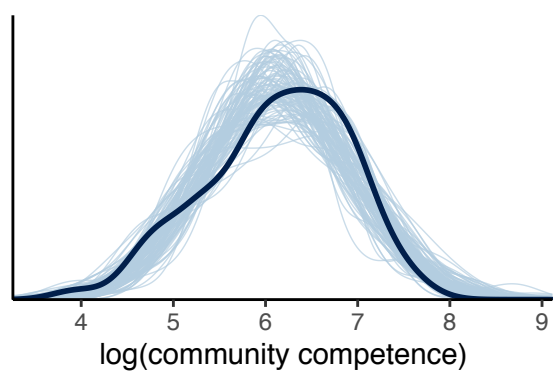

Figure B.4: Density plots of posterior predictions (100 samples, light blue) against observed (dark blue) log-community competence.
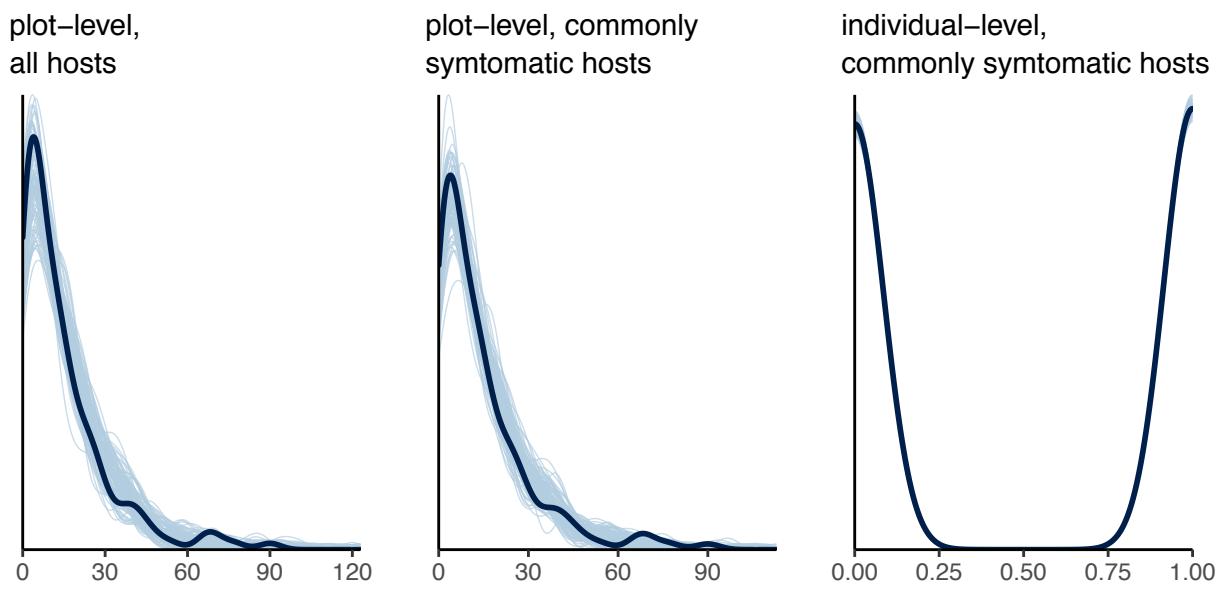
Figure B.5: Density plots of posterior predictions (100 samples, light blue) against observed infections (dark blue) from the best performing disease risk models assessed at the plot or individual level for all hosts or highly susceptible species.

Supplementary tables

Table B.1: Annotated metadata from meta-analyses testing prevalence of the dilution effect. Metadata is supplementary data from Civitello et al. (2013), Magnusson et al. (2020), and Salkeld et al. (2015). Additional columns (right of the thick black vertical line) were added to indicate whether the effect was assessed using community disease prevalence and any useful other information. Table is downloadable at https://osf.io/gzfjr/.

Table B.2: Details on species included in the study. Total basal area, number of plants, and number of infected plants are summed for each species across all plots. Hosts types are designated by the following criteria: "commonly symptomatic host"—infections were commonly detected; "rarely symptomatic host"—infections were rarely detected; and "nonhosts"—no natural *P. ramorum* infections have ever been detected.

Latin name	Plots present	Total Basal area	No. plants	No. infected plants	Host type
Umbellularia californica	112	40.7	1104	923	commonly symptomatic
Notholithocarpus densiflorus	108	60.4	2189	1153	commonly symptomatic
Sequoia sempervirens	70	274.7	746	8	rarely symptomatic
Quercus agrifolia	49	49.1	296	36	commonly symptomatic
Q. parvula	48	30.7	617	28	commonly symptomatic
Arbutus menziesii	43	26.4	418	0	rarely symptomatic
Q. chrysolepis	19	9.6	73	0	rarely symptomatic
Acer macrophyllum	18	2.1	36	0	rarely symptomatic
Toxicodendron diversilobum	18	>0.05	29	0	rarely symptomatic
Heteromeles arbutifolia	16	0.3	38	0	rarely symptomatic
Ceanothus oliganthus	9	0.4	94	0	nonhost
Lonicera hispidula	6	>0.05	7	0	rarely symptomatic
Pinus ponderosa	5	0.2	5	0	rarely symptomatic
Frangula californica	5	>0.05	35	0	rarely symptomatic
Aesculus californica	4	0.4	7	1	rarely symptomatic
Arctostaphylos sp.	3	>0.05	5	0	rarely symptomatic
Q. kelloggii	3	2.2	12	0	rarely symptomatic
Q. lobata	2	0.5	7	0	nonhost
Ceanothus sp.	1	0.2	56	0	rarely symptomatic
C. papillosus	1	>0.05	18	0	nonhost
Lathyrus vestitus	1	>0.05	1	0	nonhost
Morella cerifera	1	>0.05	1	0	nonhost
Platanus racemosa	1	0.1	1	0	nonhost
Pseudotsuga menziesii	1	0.1	1	0	rarely symptomatic
Rhamnus ilicifolia	1	>0.05	1	0	nonhost
Sambucus mexicana	1	>0.05	1	0	nonhost

Table B.3: Posterior estimates (median log-odds, 90th HDPI) of the community-level infection risk model assessed among all host species.

variable	Richness only	Richness + density of key hosts	Richness + community competency
a0	-0.2 (-0.43, 0.03)	-0.32 (-0.54, -0.09)	-0.16 (-0.37, 0.07)
Year*	-0.09 (-0.42, 0.24)	0.13 (-0.19, 0.48)	-0.05 (-0.4, 0.26)
Forest type†	-0.42 (-0.77, -0.09)	-0.36 (-0.7, -0.02)	-0.57 (-0.91, -0.24)
Host vegetative coverage	0.47 (0.14, 0.79)	0.57 (0.21, 0.88)	0.46 (0.16, 0.78)
Precipitation	-0.44 (-0.78, -0.13)	-0.17 (-0.52, 0.13)	-0.38 (-0.68, -0.08)
Potential solar induction	-0.08 (-0.4, 0.22)	-0.17 (-0.5, 0.12)	-0.19 (-0.51, 0.12)
Richness	-0.38 (-0.71, -0.1)	-0.35 (-0.66, -0.04)	-0.24 (-0.54, 0.08)
Bay laurel basal area	–	1.26 (0.9, 1.57)	–
Tanoak basal area	–	0.45 (0.1, 0.78)	–
Community competency	–	–	0.69 (0.35, 0.99)
theta	2.1 (2, 2.28)	2.34 (2, 2.7)	2.14 (2, 2.36)

* Estimate for plots sampled in 2007.

† Estimate for redwood forests.

Table B.4: Posterior estimates (median log-odds, 90th HDPI) of the community-level infection risk model assessed among commonly symptomatic species.

variable	Richness only	Richness + density of key hosts	Richness + community competency
a0	0.22 (-0.04, 0.45)	0.03 (-0.2, 0.27)	0.23 (0, 0.46)
Year*	-0.22 (-0.54, 0.13)	0.08 (-0.24, 0.44)	-0.15 (-0.49, 0.21)
Forest type†	-0.15 (-0.47, 0.22)	0.02 (-0.31, 0.39)	-0.28 (-0.62, 0.08)
Host vegetative coverage	0.42 (0.09, 0.76)	0.57 (0.21, 0.91)	0.39 (0.03, 0.71)
Precipitation	-0.73 (-1.03, -0.38)	-0.37 (-0.7, -0.01)	-0.65 (-1.01, -0.33)
Potential solar induction	-0.04 (-0.35, 0.28)	-0.1 (-0.42, 0.22)	-0.16 (-0.49, 0.17)
Richness	-0.18 (-0.5, 0.16)	-0.15 (-0.49, 0.19)	-0.02 (-0.36, 0.33)
Bay laurel basal area	–	1.43 (1.07, 1.79)	–
Tanoak basal area	–	0.3 (-0.07, 0.65)	–
Community competency	–	–	0.77 (0.41, 1.1)
theta	2.06 (2, 2.17)	2.14 (2, 2.38)	2.06 (2, 2.2)

* Estimate for plots sampled in 2007.

† Estimate for redwood forests.

Table B.5: Posterior estimates (median log-odds, 90th HDPI) of the individual-level infection risk model assessed among commonly symptomatic species.

variable	Richness only	Richness + density of key hosts	Richness + community competency
Tanoak intercept	0.83 (0.38, 1.28)	0.74 (0.33, 1.17)	0.86 (0.42, 1.29)
Coast live oak intercept	-2.23 (-2.81, -1.64)	-2.46 (-3.06, -1.84)	-2.14 (-2.76, -1.56)
Shreve oak intercept	-3.12 (-3.73, -2.44)	-3.49 (-4.15, -2.85)	-3.09 (-3.71, -2.43)
Bay laurel intercept	2.02 (1.57, 2.44)	1.63 (1.18, 2.06)	2.06 (1.63, 2.49)
Basal area of individual	0.62 (0.43, 0.79)	0.6 (0.42, 0.8)	0.6 (0.4, 0.79)
Forest type†	-0.68 (-1.24, -0.11)	-0.42 (-1, 0.12)	-0.8 (-1.4, -0.22)
Year*	-0.42 (-0.98, 0.17)	-0.13 (-0.69, 0.42)	-0.35 (-0.96, 0.19)
Precipitation	-1.47 (-2, -0.93)	-1.01 (-1.6, -0.45)	-1.42 (-1.94, -0.87)
Potential solar induction	-0.09 (-0.63, 0.44)	-0.16 (-0.7, 0.34)	-0.24 (-0.8, 0.3)
Host vegetative coverage	1.11 (0.53, 1.66)	1.39 (0.78, 1.89)	1.08 (0.53, 1.64)
Mean effect of richness	0.27 (-0.48, 1.01)	0.22 (-0.6, 1.03)	0.38 (-0.35, 1.08)
Tanoak-specific richness	-0.14 (-0.79, 0.58)	-0.48 (-1.11, 0.2)	-0.02 (-0.68, 0.66)
Coast live oak-specific richness	0.12 (-0.61, 0.94)	0.08 (-0.74, 0.81)	0.21 (-0.57, 0.97)
Shreve oak-specific richness	0.41 (-0.42, 1.35)	0.56 (-0.43, 1.45)	0.52 (-0.36, 1.45)
Bay laurel-specific richness	0.83 (0.05, 1.49)	0.97 (0.31, 1.71)	0.96 (0.21, 1.71)
Bay laurel basal area	–	1.72 (1.14, 2.34)	–
Tanoak basal area	–	-0.15 (-0.72, 0.47)	–
Community competency	–	–	0.67 (0.11, 1.21)
Species SD	2.17 (1.24, 3.45)	2.21 (1.22, 3.43)	2.16 (1.19, 3.38)
Richness slope SD	0.6 (0.05, 1.26)	0.8 (0.26, 1.57)	0.61 (0.06, 1.28)
Plot SD	1.78 (1.55, 2.01)	1.66 (1.45, 1.89)	1.78 (1.55, 2.02)

* Estimate for plots sampled in 2007.

† Estimate for redwood forests.

Additional study design and data collection details

Sample collections

As described in the main text, we collected *P. ramorum* symptom data from all stems ≥ 1 cm diameter breast height (DBH) to assess disease risk. Additionally, in each plot, samples from 3–5 plants were collected and plated onto an oomycete-selective medium (pimaricin-ampicillin-rifampicin-pentachloronitrobenzene agar; Jeffers & Martin 1986). *P. ramorum* was considered present in a plot when at least one sample matched its morphotype.

Plot selection

We focused on plots where the pathogen was confirmed present using the culture-based methods, for a total of 151 plots. Our decision to exclude culture-negative plots differs from the analysis by Haas *et al.* (2011), which analyzed disease risk from 278 plots using a zero-inflated binomial model. The zero-inflated model is a mixture model that assesses two processes: i) occurrence of the pathogen with the additional assumption that some culture-negative plots may in fact contain undetected infections, and ii) disease prevalence in culture-positive plots. Since this invasive species, *P. ramorum*, was still actively spreading to new parts of the study region during the observation period, we were interested in factors that control disease prevalence and not pathogen establishment. Thus, we analyzed culture-positive plots only. Similarly, Haas *et al.* (2011) exclusively discussed the results from the prevalence model. Their models qualitatively matched our models assessing disease prevalence among all hosts in a plot, indicating that our plot selection did not bias results. Furthermore, our individual-level models can only include plots in which the disease was present– they cannot also assess disease in a plot where the pathogen has not yet established. Considering that we contrasted disease risk at the individual and plot level, we needed to ensure consistency over which plots were used.

Plot variables

We measured the density of species using total basal area. We also considered mean basal area as an alternative density metric since larger individuals may spread more spores throughout the canopy, but we found that it strongly correlated with total basal area (Figure B.6).
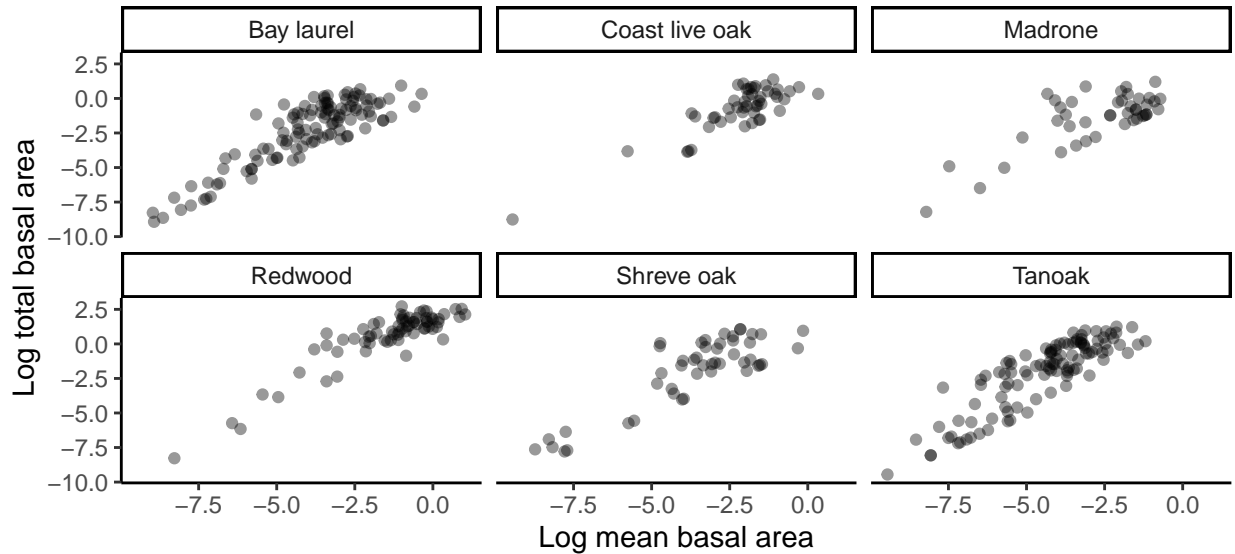
Figure B.6: Mean basal area of individuals in a plot was highly correlated with the total basal area for the top 6 most commonly occurring species. Plots with more total basal area on average had larger individual plants.

Additionally, plot diversity was characterized using species richness of woody plants with stems ≥ 1 cm DBH. In contrast, Haas *et al.* (2011) also included shrubs below the 1 cm DBH cutoff as long as the areal coverage was at least 1 m^2. Since we estimated community competence as the product of each species' mean competence and basal area, translating areal sizes of shrubs into basal area units would be inconsistent and inaccurate. As a result, we excluded shrubs below 1 cm DBH from our analysis altogether. Exploratory models showed that inclusion of these shrubs in the richness estimates led to qualitatively similar results.

Additional treatments of spatial autocorrelation

Summary

In addition to testing for spatial autocorrelation using a Moran's I correlogram (Figure B.7), we explored how our results might change if we incorporated a spatially weighted term into our models. Gaussian process (GP) regressions allow the covariance between plots to decay with distance. Because these models are computationally intensive, we ran one model assessing individual-level disease risk including covariates from the best performing non-spatial models (M2: +richness, tanoak basal area, and bay laurel basal). We also attempted to fit a GP community-level disease

risk model, but it would not converge. We suspect this is because the model was unable to seperate the two dispersion terms–the spatially weighted intercept and the dispersion parameter in the beta-binomial likelihood.
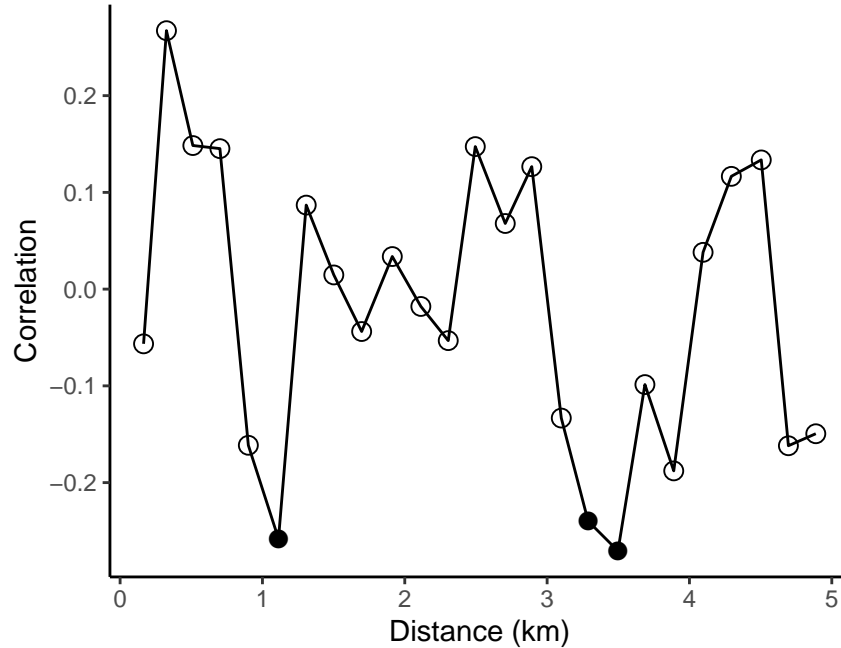

Figure B.7: Moran's I correlogram testing for spatial autocorrelation. The mean Pearson's residuals from the best performing model assessing community-level disease prevalence among all hosts were used to assess unexplained correlations between plots and their pairwise distances. Closed black circles indicate significant autocorrelation ($p < 0.05$).

The posteriors from the GP individual-level model were nearly identical to the non-GP model and predictive performance was indistinguishable ($\Delta\text{ELPD} = -0.3, \text{SE}_\Delta = 0.4$) As a result, we did not pursue the spatial models for the main analysis. Descriptions of the GP model are below.

Spatial disease risk models

The GP individual-level disease risk model was the same Bernoulli model as described in the main text (i=individual observation, j=plot, and s=species), except that the plot-level intercept spatially varied:

$$I_i \sim \text{Bernoulli}(p_i)$$

$$\text{logit}(p_i) = \alpha_{j[i]} + \alpha_{s[i]} + \beta_{s[i]} richness_{j[i]} + \gamma BA_i$$

$$\alpha_j \sim \text{MVNormal}(BX_j, \ K(d))$$

$$[K(d)]_{m,n} = \eta^2 \exp(-\frac{1}{2\rho^2}(d_{mn})^2) + I(m = n)\sigma^2$$

$$\begin{bmatrix} \alpha_s \\ \beta_s \end{bmatrix} \sim \text{MVNormal}\Big(\begin{bmatrix} \alpha_0 \\ \bar{\beta} \end{bmatrix}, \ \boldsymbol{\Sigma} \Big).$$

The covariance matrix $K(d)$ of the plot-varying intercept (α_j) was defined by an exponentiated quadratic kernel. This function decayed with distance between plots m and n and its range and intensity were controlled by ρ^2 and η^2, respectively. The term σ^2 accounted for repeated plot observations (i.e. when plot $m = n$).

Correlation between plots

Using the posteriors from the GP individual-level model, we show the correlation between plots as a function of distance (Figure B.8). Spatial autocorrelation was only noticeable at very short distances, primarily between plots less than 1.25 km apart.
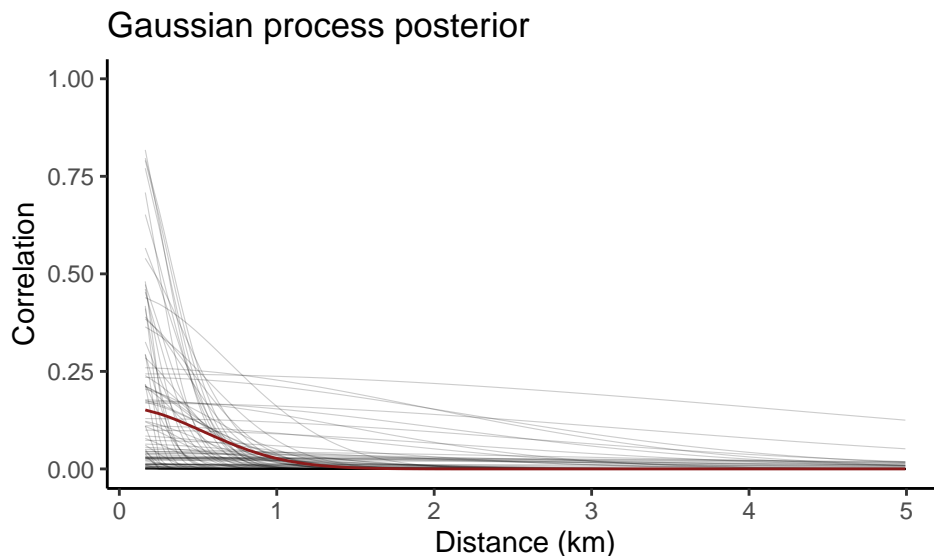

Figure B.8: Median (red) correlation between plots with 100 posterior draws (grey).

Only 2% of the pairwise distances between plots were within 1.25 km of each other (Figure B.9). It is possible that the GP models were similar to the non-GP models because there were so

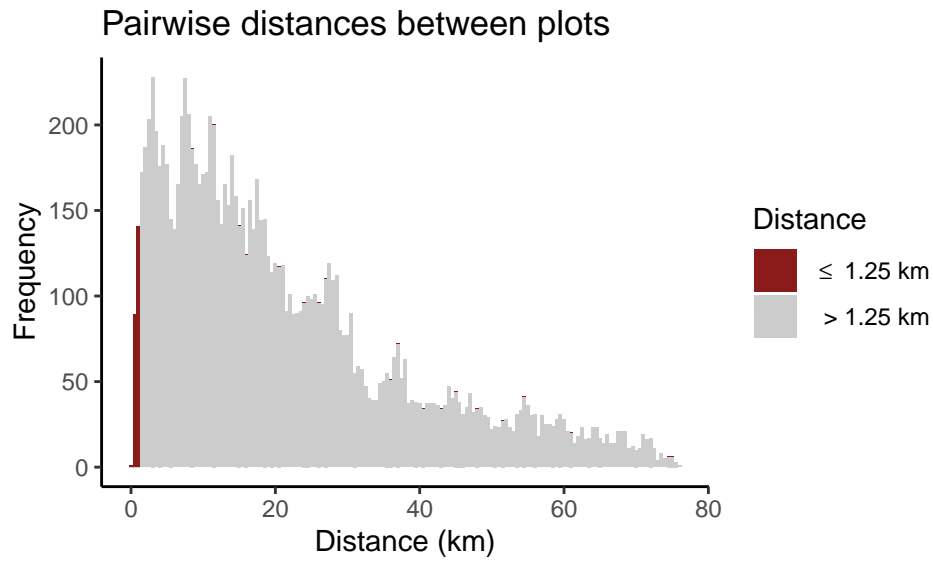few plots where spatial autocorrelation was of potential concern.

Figure B.9: Distribution of plot pairwise distances.

R Packages

For fitting, visualizing, summarizing, and contrasting Bayesian models, we used `Rstan`, `rethinking`, `Bayesplot`, and `loo` (Yao *et al.* 2017; Gabry *et al.* 2019; McElreath 2020; Stan Development Team 2020). For data wrangling and creating figures, we used `dplyr`, `ggplot2`, and `cowplot` (Wickham 2016; Wilke 2019; Wickham *et al.* 2021).
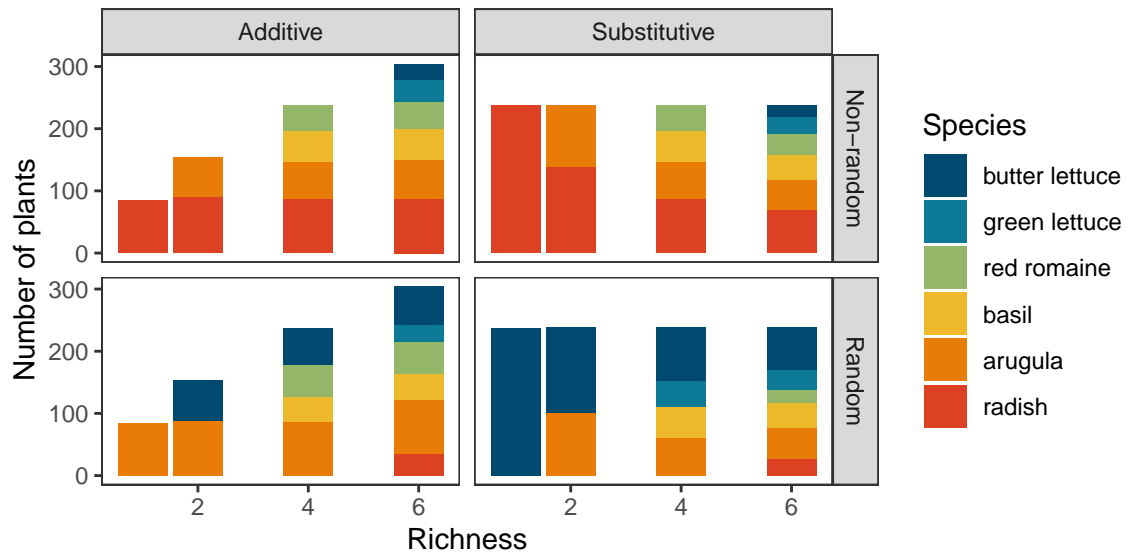
Figure C.1: Depiction of experimental design for the 4 treatments. Note that for each series of communities (four trays along the richness gradient), the order of assembling species was the same in the 'non-random' treatments, and different in the 'random' treatments.
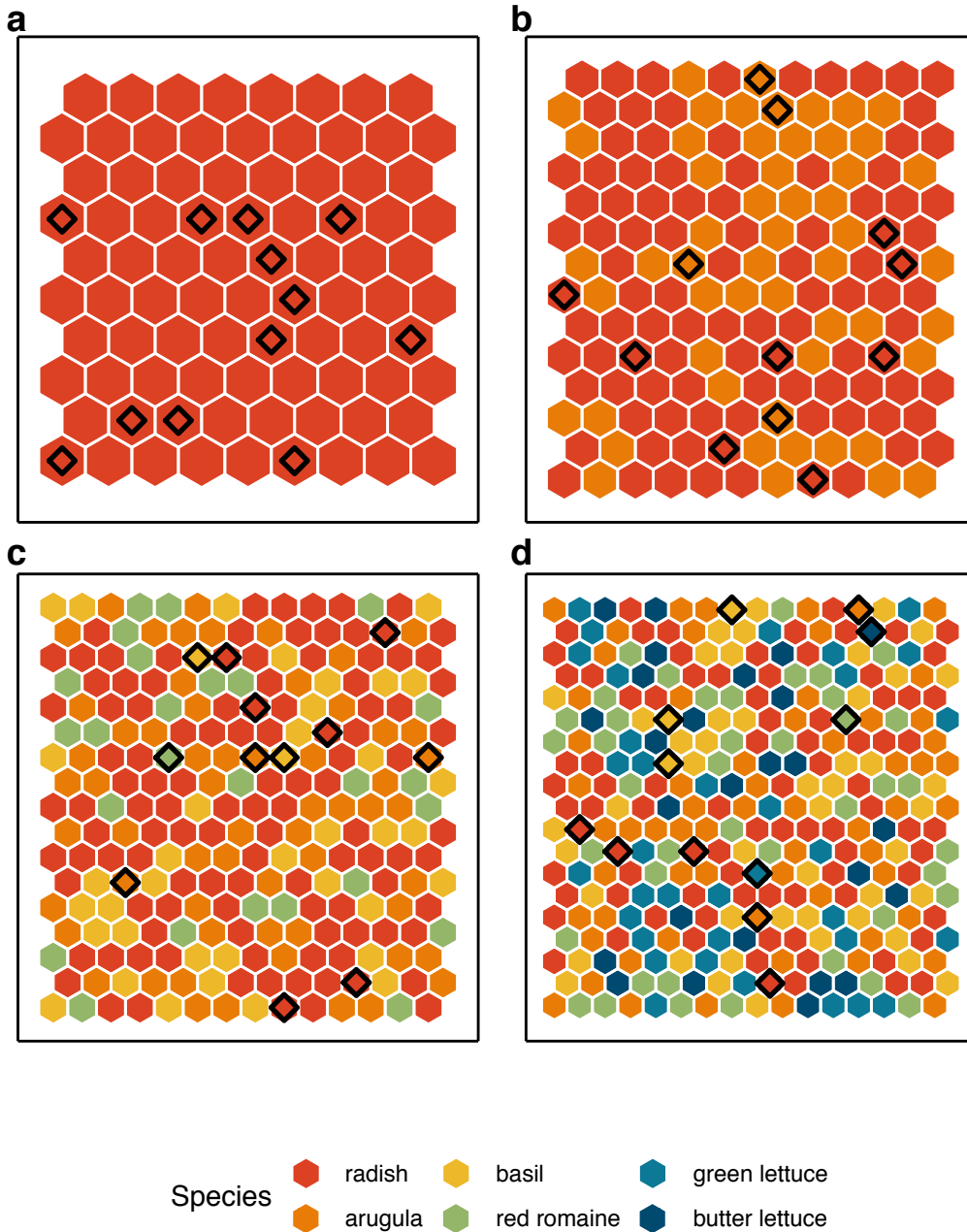
Figure C.2: Spatial depiction of a series of trays with richness levels 1, 2, 4, and 6 (a–d respectively). Colors represent planted species and black diamonds indicate plants that were inoculated with the pathogen. This series of trays represent an additive/non-random assembly treatment.
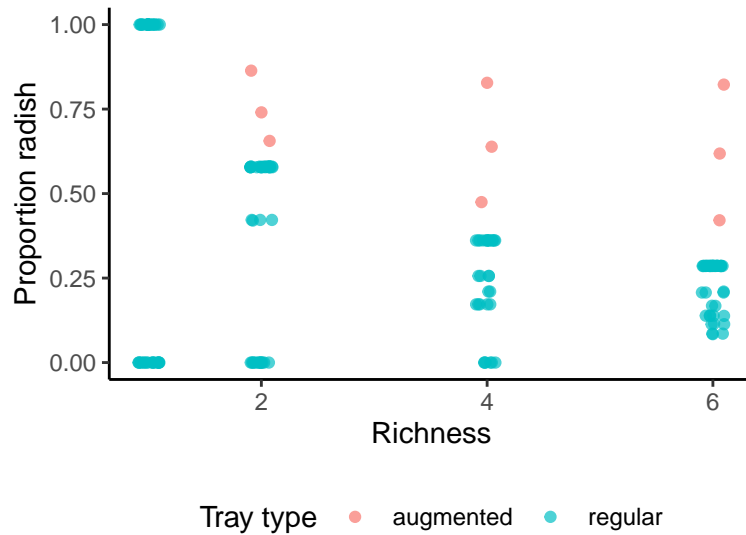
Figure C.3: Extra trays ('augmented' trays) were planted to mitigate the negative correlation between richness and radish, inherent from the experimental design ('regular' trays).
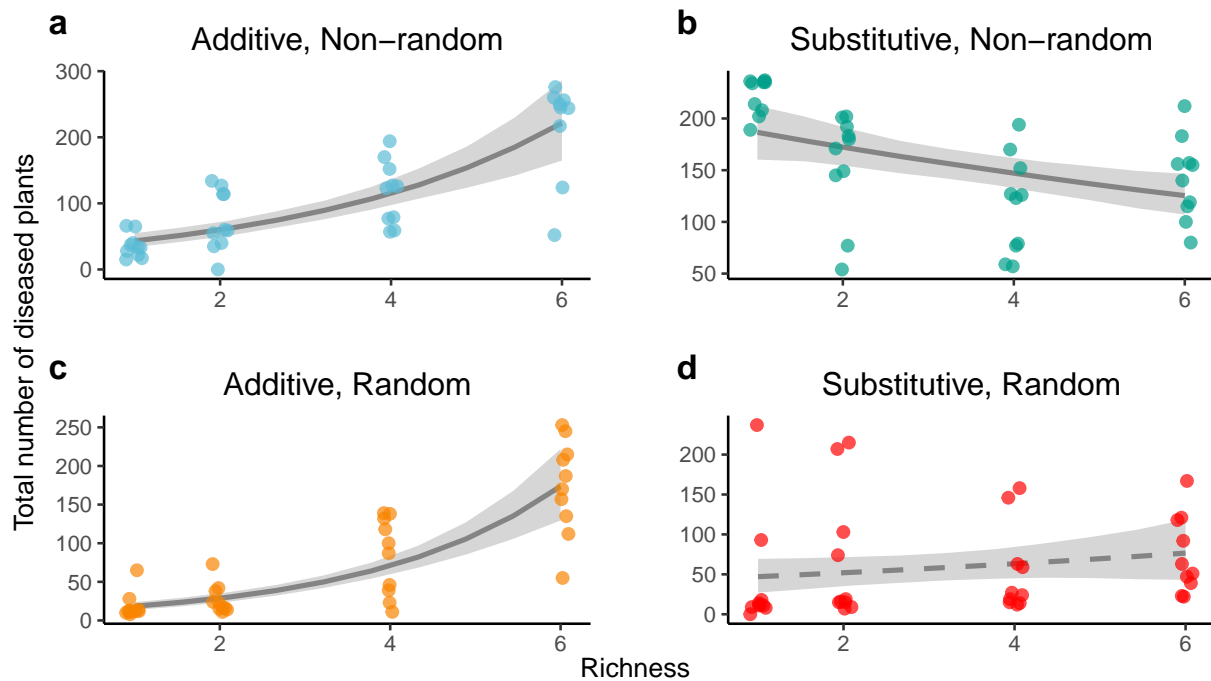
Figure C.4: Relationships between richness and total density of diseased individuals for different community assembly patterns. Lines and shaded regions represent the median and 90% HPDI of the posterior estimate of the mean. Solid lines indicate the 90% HPDI of the coefficient of richness did not contain zero.

Table C.1: Posterior estimates (median log-odds, 90th HPDI) of the contrasting species-level disease risk models. All models included species-varying intercepts and coefficients of richness, terms for day planted and soil temperature, and a tray-varying intercept. Additional covariates are listed in the first column.

Tray-level covariates[*]	richness	Radish density	Arugula density	Density of other species[†]	ΔELPD	SE_Δ
D + R + A	0.47 (-0.26, 1.17)	3.32 (2.65, 3.99)	0.71 (0.13, 1.34)	0.43 (-0.37, 1.24)	0	0
R + A + B + Re + G + Bu	-0.07 (-1.18, 1.01)	3.45 (2.73, 4.15)	0.8 (0.23, 1.36)	–	-4.3	8.5
D + R	0.4 (-0.21, 0.99)	3.74 (3.01, 4.42)	–	0.98 (0.19, 1.72)	-9.2	7.7
D	0.88 (0.15, 1.58)	–	–	1.21 (0.50, 1.93)	-40.9	8.6

[*] Codes for covariates: R = radish, A = arugula, B = basil, Re = red romaine, G = green lettuce, Bu = butter lettuce, D = density

[†] When individual species were incorporated as covariates in the model, density ('D') represents the cumulative density of other species. When no individual species was incorporated, 'D' represents density of all species.

References

Almeida-Neto, M., Guimaraes, P., Guimaraes, P.R., Jr, Loyola, R.D. & Ulrich, W. (2008). A consistent metric for nestedness analysis in ecological systems: reconciling concept and measurement. *Oikos*, 117, 1227–1239.

Bailey, D.J., Otten, W. & Gilligan, C.A. (2000). Saprotrophic invasion by the soil-borne fungal plant pathogen Rhizoctonia solani and percolation thresholds. *New Phytol.*, 146, 535–544.

Bradley, C.A., Gibbs, S.E.J. & Altizer, S. (2008). Urban land use predicts West Nile virus exposure in songbirds. *Ecol. Appl.*, 18, 1083–1092.

Brown, M.V., Moore, J.N., Fenn, P. & McNew, R.W. (1999). Comparison of Leaf Disk, Greenhouse, and Field Screening Procedures for Evaluation of Grape Seedlings for Downy Mildew Resistance. *HortScience*, 34, 331–333.

Bürkner, P.-C. (2017). **brms**: An *R* Package for Bayesian Multilevel Models Using *Stan*. *J. Stat. Softw.*, 80.

Cardinale, B.J., Duffy, J.E., Gonzalez, A., Hooper, D.U., Perrings, C. & Venail, P. *et al.* (2012). Biodiversity loss and its impact on humanity. *Nature*, 486, 59–67.

Civitello, D.J., Cohen, J., Fatima, H., Halstead, N.T., Liriano, J. & McMahon, T.A. *et al.* (2015). Biodiversity inhibits parasites: broad evidence for the dilution effect. *Proc. Natl. Acad. Sci. USA*, 112, 8667–8671.

Cobb, R.C., Chan, M.N., Meentemeyer, R.K. & Rizzo, D.M. (2012a). Common factors drive disease and coarse woody debris dynamics in forests impacted by sudden oak death. *Ecosystems*, 15, 242–255.

Cobb, R.C., Filipe, J.A.N., Meentemeyer, R.K., Gilligan, C.A. & Rizzo, D.M. (2012b). Ecosystem transformation by emerging infectious disease: loss of large tanoak from California forests: *Ecosystem transformation by disease*. *J. Ecol.*, 100, 712–722.

Cobb, R.C., Haas, S.E., Kruskamp, N., Dillon, W.W., Swiecki, T.J. & Rizzo, D.M. *et al.* (2020). The magnitude of regional-scale tree mortality caused by the invasive pathogen *Phytophthora ramorum*. *Earth's Future*, 8, e2020EF001500.

Cobb, R.C., Meentemeyer, R.K. & Rizzo, D.M. (2010). Apparent competition in canopy trees determined by pathogen transmission rather than susceptibility. *Ecology*, 91, 327–333.

Cobb, R.C., Rizzo, D.M., Hayden, K.J., Garbelotto, M., Filipe, J.A.N. & Gilligan, C.A. *et al.* (2013). Biodiversity Conservation in the Face of Dramatic Forest Disease: An Integrated Conservation Strategy for Tanoak (*Notholithocarpus densiflorus*) Threatened by Sudden Oak Death. *Madroño*, 60, 151–164.

Cobb, R., Hartsough, P., Ross, N., Klein, J., LaFever, D. & Frankel, S. *et al.* (2017). Resiliency or restoration: management of sudden oak death before and after outbreak. *For Phytophthoras*, 7.

Cohen, R. (1993). A Leaf Disk Assay for Detection of Resistance of Melons to *Sphaerotheca fuliginea*

Race 1. *Plant Disease*, 77, 513–517.

Cronin, J.P., Welsh, M.E., Dekkers, M.G., Abercrombie, S.T. & Mitchell, C.E. (2010). Host physiological phenotype explains pathogen reservoir potential: epidemiology and host physiology. *Ecol. Lett.*, 13, 1221–1232.

Cunniffe, N.J., Cobb, R.C., Meentemeyer, R.K., Rizzo, D.M. & Gilligan, C.A. (2016). Modeling when, where, and how to manage a forest epidemic, motivated by sudden oak death in California. *Proc. Natl. Acad. Sci. U. S. A.*, 113, 5640–5645.

Daly, C., Neilson, R.P. & Phillips, D.L. (1994). A statistical-topographic model for mapping climatological precipitation over mountainous terrain. *J. Appl. Meteorol.*, 33, 140–158.

Davidson, J.M., Patterson, H.A. & Rizzo, D.M. (2008). Sources of inoculum for *Phytophthora ramorum* in a redwood forest. *Phytopathology*, 98, 860–866.

Davidson, J.M., Patterson, H.A., Wickland, A.C., Fichtner, E.J. & Rizzo, D.M. (2011). Forest type influences transmission of *Phytophthora ramorum* in California oak woodlands. *Phytopathology*, 101, 492–501.

Davidson, J.M., Werres, S., Garbelotto, M., Hansen, E.M. & Rizzo, D.M. (2003). Sudden oak death and associated diseases caused by *Phytophthora ramorum*. *Plant Health Prog.*, 4.

Davidson, J.M., Wickland, A.C., Patterson, H.A., Falk, K.R. & Rizzo, D.M. (2005). Transmission of *Phytophthora ramorum* in mixed-evergreen forest in California. *Phytopathology*, 95, 587–596.

Denman, S., Kirk, S.A., Brasier, C.M. & Webber, J.F. (2005). In vitro leaf inoculation studies as an indication of tree foliage susceptibility to Phytophthora ramorum in the UK. *Plant Pathol.*, 54, 512–521.

Denman, S., Kirk, S.A., Moralejo, E. & Webber, J.F. (2009). *Phytophthora ramorum* and *Phytophthora kernoviae* on naturally infected asymptomatic foliage. *EPPO Bulletin*, 39, 105–111.

Dillon, W.W. & Meentemeyer, R.K. (2019). Direct and indirect effects of forest microclimate on pathogen spillover. *Ecology*, 100, e02686.

Dodd, R.S., Hüberli, D., Douhovnikoff, V., Harnik, T.Y., Afzal-Rafii, Z. & Garbelotto, M. (2005). Is variation in susceptibility to Phytophthora ramorum correlated with population genetic structure in coast live oak (Quercus agrifolia)? *New Phytol.*, 165, 203–214.

Dodd, R.S., Hüberli, D., Mayer, W., Harnik, T.Y., Afzal-Rafii, Z. & Garbelotto, M. (2008). Evidence for the role of synchronicity between host phenology and pathogen activity in the distribution of sudden oak death canker disease. *New Phytol.*, 179, 505–514.

Dubayah, R. & Rich, P.M. (1995). Topographic solar radiation models for GIS. *International journal of geographical information systems*, 9, 405–419.

Fichtner, E.J., Lynch, S.C. & Rizzo, D.M. (2007). Detection, Distribution, Sporulation, and Survival of *Phytophthora ramorum* in a California Redwood-Tanoak Forest Soil. *Phytopathology*, 97, 1366–1375.

Fichtner, E.J., Lynch, S.C. & Rizzo, D.M. (2009). Survival, Dispersal, and Potential Soil-Mediated Suppression of *Phytophthora ramorum* in a California Redwood-Tanoak Forest. *Phytopathology*, 99, 608–619.

Fukami, T., Martijn Bezemer, T., Mortimer, S.R. & Putten, W.H. (2005). Species divergence and trait convergence in experimental plant community assembly. *Ecol. Lett.*, 8, 1283–1290.

Gabry, J., Simpson, D., Vehtari, A., Betancourt, M. & Gelman, A. (2019). Visualization in Bayesian workflow. *J. R. Stat. Soc. Ser. A Stat. Soc.*, 182, 389–402.

Garbelotto, M., Davidson, J.M., Ivors, K., Maloney, P.E., Hüberli, D. & Koike, S.T. *et al.* (2003). Non-oak native plants are main hosts for sudden oak death pathogen in California. *Calif. Agric.*, 57, 18–23.

Garbelotto, M., Schmidt, D., Swain, S., Hayden, K. & Lione, G. (2017). The ecology of infection between a transmissive and a dead-end host provides clues for the treatment of a plant disease. *Ecosphere*, 8, e01815.

Gelman, A. (2008). Scaling regression inputs by dividing by two standard deviations. *Stat. Med.*, 27, 2865–2873.

Gibb, R., Redding, D.W., Chin, K.Q., Donnelly, C.A., Blackburn, T.M. & Newbold, T. *et al.* (2020). Zoonotic host diversity increases in human-dominated ecosystems. *Nature*, 584, 398–402.

Goodrich, B., Gabry, J., Ali, I. & Brilleman, S. (2020). *rstanarm: Bayesian applied regression modeling via Stan.*

Grünwald, N.J., LeBoldus, J.M. & Hamelin, R.C. (2019). Ecology and Evolution of the Sudden Oak Death Pathogen *Phytophthora ramorum. Annu. Rev. Phytopathol.*, 57, 301–321.

Guilherme Becker, C. & Zamudio, K.R. (2011). Tropical amphibian populations experience higher disease risk in natural habitats. *Proc. Natl. Acad. Sci. U. S. A.*

Guo, Q., Shaffer, T. & Buhl, T. (2006). Community maturity, species saturation and the variant diversity?productivity relationships in grasslands. *Ecol. Lett.*, 9, 1284–1292.

Haas, S.E., Cushman, J.H., Dillon, W.W., Rank, N.E., Rizzo, D.M. & Meentemeyer, R.K. (2015). Effects of Individual, Community and Landscape Drivers on the Dynamics of a Wildland Forest Epidemic. *Ecology*, 15–0767.1.

Haas, S.E., Hooten, M.B., Rizzo, D.M. & Meentemeyer, R.K. (2011). Forest species diversity reduces disease risk in a generalist plant pathogen invasion. *Ecol. Lett.*, 14, 1108–1116.

Halliday, F.W., Heckman, R.W., Wilfahrt, P.A. & Mitchell, C.E. (2019). Past is prologue: host community assembly and the risk of infectious disease over time. *Ecol. Lett.*, 22, 138–148.

Halliday, F.W. & Rohr, J.R. (2019). Measuring the shape of the biodiversity-disease relationship across systems reveals new findings and key gaps. *Nat. Commun.*, 10, 5032.

Halsey, S. (2019). Defuse the dilution effect debate. *Nature Ecology & Evolution*, 3, 145–146.

Hamer, G.L., Chaves, L.F., Anderson, T.K., Kitron, U.D., Brawn, J.D. & Ruiz, M.O. *et al.* (2011). Fine-scale variation in vector host use and force of infection drive localized patterns of West Nile virus transmission. *PLoS One*, 6, e23767.

Hansen, E.M., Kanaskie, A., Prospero, S., McWilliams, M., Goheen, E.M. & Osterbauer, N. *et al.* (2008). Epidemiology of *Phytophthora ramorum* in Oregon tanoak forests. *Can. J. For. Res.*,

38, 1133–1143.

Hansen, E.M., Parke, J.L. & Sutton, W. (2005). Susceptibility of Oregon Forest Trees and Shrubs to *Phytophthora ramorum*: A Comparison of Artificial Inoculation and Natural Infection. *Plant Dis.*, 89, 63–70.

Hantsch, L., Braun, U., Scherer-Lorenzen, M. & Bruelheide, H. (2013). Species richness and species identity effects on occurrence of foliar fungal pathogens in a tree diversity experiment. *Ecosphere*, 4, art81.

Harris, A.R. & Webber, J.F. (2016). Sporulation potential, symptom expression and detection of *Phytophthora ramorum* on larch needles and other foliar hosts. *Plant Pathol.*, 65, 1441–1451.

Harrison, J.G. & Lowe, R. (1989). Effects of humidity and air speed on sporulation of Phytophthora infestans on potato leaves. *Plant Pathol.*, 38, 585–591.

Hayden, K.J., Nettel, A., Dodd, R.S. & Garbelotto, M. (2011). Will all the trees fall? Variable resistance to an introduced forest disease in a highly susceptible host. *For. Ecol. Manage.*, 261, 1781–1791.

Heckman, R.W., Halliday, F.W. & Mitchell, C.E. (2019). A growth–defense trade-off is general across native and exotic grasses. *Oecologia*, 191, 609–620.

Hüberli, D., Hayden, K.J., Calver, M. & Garbelotto, M. (2012). Intraspecific variation in host susceptibility and climatic factors mediate epidemics of sudden oak death in western US forests: Susceptibility variation of bay laurel to sudden oak death. *Plant Pathol.*, 61, 579–592.

Hüberli, D., Lutzy, B., Voss, B., Calver, M., Ormsby, M. & Garbelotto, M. (2008). Susceptibility of New Zealand flora to *Phytophthora ramorum* and pathogen sporulation potential: an approach based on the precautionary principle. *Australas. Plant Pathol.*, 37, 615.

Hydeman, M.E., Longo, A.V., Velo-Antón, G., Rodriguez, D., Zamudio, K.R. & Bell, R.C. (2017). Prevalence and genetic diversity of Batrachochytrium dendrobatidis in Central African island and continental amphibian communities. *Ecol. Evol.*, 7, 7729–7738.

Ireland, K.B., Hüberli, D., Dell, B., Smith, I.W., Rizzo, D.M. & Hardy, G.E.S.J. (2012). Potential susceptibility of Australian flora to a NA2 isolate of Phytophthora ramorum and pathogen sporulation potential: Australian plant susceptibility to P. ramorum. *For. Pathol.*, 42, 305–320.

Jeffers, S.N. & Martin, S.B. (1986). Comparison of two media selective for Phytophthora and Pythium species. *Plant Dis.*

Jinek, A., Simard, M., Brière, S.C., Watson, A.K., Tweddell, R.J. & Rioux, D. (2011). Foliage susceptibility of six eastern Canadian forest tree species to *Phytophthora ramorum. Can. J. Plant Pathol.*, 33, 26–37.

Johnson, P.T.J., Calhoun, D.M., Riepe, T., McDevitt-Galles, T. & Koprivnikar, J. (2019). Community disassembly and disease: realistic—but not randomized—biodiversity losses enhance parasite transmission. *Proc. R. Soc. B.*, 286, 20190260.

Johnson, P.T.J., Ostfeld, R.S. & Keesing, F. (2015a). Frontiers in research on biodiversity and disease. *Ecol. Lett.*, 18, 1119–1133.

Johnson, P.T.J., Preston, D.L., Hoverman, J.T., Henderson, J.S., Paull, S.H. & Richgels, K.L.D. *et al.* (2012). Species diversity reduces parasite infection through cross-generational effects on host abundance. *Ecology*, 93, 56–64.

Johnson, P.T.J., Preston, D.L., Hoverman, J.T. & Richgels, K.L.D. (2013). Biodiversity decreases disease through predictable changes in host community competence. *Nature*, 494, 230–233.

Johnson, P.T.J., Roode, J.C. de & Fenton, A. (2015b). Why infectious disease research needs community ecology. *Science*, 349, 1259504–1259504.

Joseph, M.B., Mihaljevic, J.R., Orlofske, S.A. & Paull, S.H. (2013). Does life history mediate changing disease risk when communities disassemble? *Ecol. Lett.*, 16, 1405–1412.

Keesing, F., Holt, R.D. & Ostfeld, R.S. (2006). Effects of species diversity on disease risk. *Ecol. Lett.*, 9, 485–498.

Kortekamp, A. (2006). Expression analysis of defence-related genes in grapevine leaves after inoculation with a host and a non-host pathogen. *Plant Physiol. Biochem.*, 44, 58–67.

Lacroix, C., Jolles, A., Seabloom, E.W., Power, A.G., Mitchell, C.E. & Borer, E.T. (2014). Non-random biodiversity loss underlies predictable increases in viral disease prevalence. *J. R. Soc. Interface*, 11, 20130947.

Linderman, R.G. & Davis, E.A. (2007). Comparative Host Susceptibility and Sporulation Potential of *Phytophthora ramorum*. *Plant Health Prog.*, 8, 15.

Liu, X., Chen, F., Lyu, S., Sun, D. & Zhou, S. (2018). Random species loss underestimates dilution effects of host diversity on foliar fungal diseases under fertilization. *Ecol. Evol.*, 8, 1705–1713.

Liu, X., Chen, L., Liu, M., Garcı'a-Guzmán, G., Gilbert, G.S. & Zhou, S. (2020). Dilution effect of plant diversity on infectious diseases: latitudinal trend and biological context dependence. *Oikos*, 129, 457–465.

Luis, A.D., Kuenzi, A.J. & Mills, J.N. (2018). Species diversity concurrently dilutes and amplifies transmission in a zoonotic host–pathogen system through competing mechanisms. *Proc. Natl. Acad. Sci. USA*, 115, 7979–7984.

Magnusson, M., Fischhoff, I.R., Ecke, F., Hörnfeldt, B. & Ostfeld, R.S. (2020). Effect of spatial scale and latitude on diversity–disease relationships. *Ecology*, 101, e02955.

Mascheretti, S., Croucher, P.J.P., Vettraino, A., Prospero, S. & Garbelotto, M. (2008). Reconstruction of the Sudden Oak Death epidemic in California through microsatellite analysis of the pathogen Phytophthora ramorum. *Mol. Ecol.*, 17, 2755–2768.

McElreath, R. (2020). *rethinking: Statistical Rethinking book package.*

Meentemeyer, R.K., Anacker, B.L., Mark, W. & Rizzo, D.M. (2008a). Early detection of emerging forest disease using dispersal estimation and ecological niche modeling. *Ecol. Appl.*, 18, 377–390.

Meentemeyer, R.K., Cunniffe, N.J., Cook, A.R., Filipe, J.A.N., Hunter, R.D. & Rizzo, D.M. *et al.* (2011). Epidemiological modeling of invasion in heterogeneous landscapes: spread of sudden oak death in California (1990–2030). *Ecosphere*, 2, art17.

Meentemeyer, R.K., Rank, N.E., Shoemaker, D.A., Oneal, C.B., Wickland, A.C. & Frangioso, K.M. *et al.* (2008b). Impact of sudden oak death on tree mortality in the Big Sur ecoregion of California. *Biol. Invasions*, 10, 1243–1255.

Meentemeyer, R., Rizzo, D., Mark, W. & Lotz, E. (2004). Mapping the risk of establishment and spread of sudden oak death in California. *For. Ecol. Manage.*, 200, 195–214.

Metz, M.R., Frangioso, K.M., Meentemeyer, R.K. & Rizzo, D.M. (2011). Interacting disturbances: wildfire severity affected by stage of forest disease invasion. *Ecol. Appl.*, 21, 313–320.

Metz, M.R., Frangioso, K.M., Wickland, A.C., Meentemeyer, R.K. & Rizzo, D.M. (2012). An emergent disease causes directional changes in forest species composition in coastal California. *Ecosphere*, 3, art86.

Metz, M.R., Varner, J.M., Frangioso, K.M., Meentemeyer, R.K. & Rizzo, D.M. (2013). Unexpected redwood mortality from synergies between wildfire and an emerging infectious disease. *Ecology*, 94, 2152–2159.

Mihaljevic, J.R., Joseph, M.B., Orlofske, S.A. & Paull, S.H. (2014). The scaling of host density with richness affects the direction, shape, and detectability of diversity-disease relationships. *PLoS One*, 9, e97812.

Milholland, M.T., Castro-Arellano, I., Arellano, E., Nava-Garcı'a, E., Rangel-Altamirano, G. & Gonzalez-Cozatl, F.X. *et al.* (2017). Species Identity Supersedes the Dilution Effect Concerning Hantavirus Prevalence at Sites across Texas and México. *ILAR J.*, 58, 401–412.

Mitchell, C.E., Tilman, D. & Groth, J.V. (2002). Effects of grassland plant species diversity, abundance, and composition on foliar fungal disease. *Ecology*, 83, 713–1726.

Moore, S.M. & Borer, E.T. (2012). The influence of host diversity and composition on epidemiological patterns at multiple spatial scales. *Ecology*, 93, 1095–1105.

Ndeffo Mbah, M.L. & Gilligan, C.A. (2010). Optimization of control strategies for epidemics in heterogeneous populations with symmetric and asymmetric transmission. *J. Theor. Biol.*, 262, 757–763.

Orłowska, E., Basile, A., Kandzia, I., Llorente, B., Kirk, H.G. & Cvitanich, C. (2012). Revealing the importance of meristems and roots for the development of hypersensitive responses and full foliar resistance to Phytophthora infestans in the resistant potato cultivar Sarpo Mira. *J. Exp. Bot.*, 63, 4765–4779.

Ostfeld, R.S. & Keesing, F. (2000). The function of biodiversity in the ecology of vector-borne zoonotic diseases. *Can. J. Zool.*, 78, 2061–2078.

Ostfeld, R.S. & Keesing, F. (2012). Effects of host diversity on infectious disease. *Annu. Rev. Ecol. Evol. Syst.*, 43, 157–182.

Ostfeld, R.S. & LoGiudice, K. (2003). Community disassembly, biodiversity loss, and the erosion of an ecosystem service. *Ecology*, 84, 1421–1427.

Otten, W., Filipe, J.A.N., Bailey, D.J. & Gilligan, C.A. (2003). Quantification and analysis of transmission rates for soilborne epidemics. *Ecology*, 84, 3232–3239.

Otten, W., Filipe, J.A.N. & Gilligan, C.A. (2005). Damping-off epidemics, contact structure, and

disease transmission in mixed-species populations. *Ecology*, 86, 1948–1957.

Otten, W., Hall, D., Harris, K., Ritz, K., Young, I.M. & Gilligan, C.A. (2001). Soil Black-wellScienceLtd physics, fungal epidemiology and the spread of. *New Phytol.*, 10.

Paulitz, T.C. & Schroeder, K.L. (2005). A New Method for the Quantification of *Rhizoctonia solani* and *R. oryzae* from Soil. *Plant Dis.*, 89, 767–772.

Peterson, E., Hansen, E. & Hulbert, J. (2014). Source or sink? The role of soil and water borne inoculum in the dispersal of Phytophthora ramorum in Oregon tanoak forests. *For. Ecol. Manage.*, 322, 48–57.

Piudo, L., Monteverde, M.J., Walker, R.S. & Douglass, R.J. (2011). Rodent community structure and Andes virus infection in sylvan and peridomestic habitats in northwestern Patagonia, Argentina. *Vector Borne Zoonotic Dis.*, 11, 315–324.

R Core Team. (2019). R: A Language and Environment for Statistical Computing.

Rizzo, D.M. & Garbelotto, M. (2003). Sudden oak death: endangering California and Oregon forest ecosystems. *Front. Ecol. Environ.*, 1, 197–204.

Rizzo, D.M., Garbelotto, M. & Hansen, E.M. (2005). *Phytophthora ramorum*: integrative research and management of an emerging pathogen in California and Oregon forests. *Annu. Rev. Phytopathol.*, 43, 309–335.

Roberts, M.G. & Heesterbeek, J.A.P. (2018). Quantifying the dilution effect for models in ecological epidemiology. *J. R. Soc. Interface*, 15, 20170791.

Roche, B., Dobson, A.P., Guégan, J.-F. & Rohani, P. (2012). Linking community and disease ecology: the impact of biodiversity on pathogen transmission. *Philos. Trans. R. Soc. Lond. B Biol. Sci.*, 367, 2807–2813.

Rohr, J.R., Civitello, D.J., Halliday, F.W., Hudson, P.J., Lafferty, K.D. & Wood, C.L. *et al.* (2020). Towards common ground in the biodiversity–disease debate. *Nat Ecol Evol*, 4, 24–33.

Rosenthal, L.M., Fajardo, S.N. & Rizzo, D. (in press). Sporulation potential of *Phytophthora ramorum* differs among common California plant species in the Big Sur region. *Plant Dis.*

Rosenthal, L.M., Simler-Williamson, A.B. & Rizzo, D.M. (in press). Community-level prevalence of a forest pathogen, not individual-level disease risk, declines with tree diversity. *Ecol. Lett.*

Rudolf, V.H.W. & Antonovics, J. (2005). Species coexistence and pathogens with frequency-dependent transmission. *Am. Nat.*, 166, 112–118.

Salkeld, D.J. & Antolin, M.F. (2020). Ecological Fallacy and Aggregated Data: A Case Study of Fried Chicken Restaurants, Obesity and Lyme Disease. *Ecohealth*, 17, 4–12.

Salkeld, D.J., Padgett, K.A. & Jones, J.H. (2013). A meta-analysis suggesting that the relationship between biodiversity and risk of zoonotic pathogen transmission is idiosyncratic. *Ecol. Lett.*, 16, 679–686.

Schmeller, D.S., Blooi, M., Martel, A., Garner, T.W.J., Fisher, M.C. & Azemar, F. *et al.* (2014). Microscopic Aquatic Predators Strongly Affect Infection Dynamics of a Globally Emerged Pathogen. *Curr. Biol.*, 24, 176–180.

Searle, C.L., Cortez, M.H., Hunsberger, K.K., Grippi, D.C., Oleksy, I.A. & Shaw, C.L. *et al.* (2016). Population density, not host competence, drives patterns of disease in an invaded community. *Am. Nat.*, 188, 554–566.

Simler, A.B., Metz, M.R., Frangioso, K.M., Meentemeyer, R.K. & Rizzo, D.M. (2018). Novel disturbance interactions between fire and an emerging disease impact survival and growth of resprouting trees. *Ecology*, 99, 2217–2229.

Simler-Williamson, A.B., Metz, M.R., Frangioso, K.M., Meentemeyer, R.K. & Rizzo, D.M. (2019). Compound disease and wildfire disturbances alter opportunities for seedling regeneration in resprouter-dominated forests. *Ecosphere*, 10.

Simler-Williamson, A.B., Metz, M.R., Frangioso, K.M. & Rizzo, D.M. (2021). Wildfire alters the disturbance impacts of an emerging forest disease via changes to host occurrence and demographic structure. *J. Ecol.*, 109, 676–691.

Simpson, E.H. (1951). The interpretation of interaction in contingency tables. *J. R. Stat. Soc.*, 13, 238–241.

Stan Development Team. (2019). Stan modeling language users guide and reference manual.

Stan Development Team. (2020). RStan: the R interface to Stan.

Stephens, P.R., Altizer, S., Smith, K.F., Alonso Aguirre, A., Brown, J.H. & Budischak, S.A. *et al.* (2016). The macroecology of infectious diseases: a new perspective on global-scale drivers of pathogen distributions and impacts. *Ecol. Lett.*, 19, 1159–1171.

Stewart Merrill, T.E. & Johnson, P.T.J. (2020). Towards a mechanistic understanding of competence: a missing link in diversity–disease research. *Parasitology*, 147, 1159–1170.

Strauss, A.T., Bowling, A.M., Duffy, M.A., Cáceres, C.E. & Hall, S.R. (2018). Linking host traits, interactions with competitors and disease: Mechanistic foundations for disease dilution. *Funct. Ecol.*, 32, 1271–1279.

Strauss, A.T., Civitello, D.J., Cáceres, C.E. & Hall, S.R. (2015). Success, failure and ambiguity of the dilution effect among competitors. *Ecol. Lett.*, 18, 916–926.

Strauss, A.T., Shocket, M.S., Civitello, D.J., Hite, J.L., Penczykowski, R.M. & Duffy, M.A. *et al.* (2016). Habitat, predators, and hosts regulate disease in Daphnia through direct and indirect pathways. *Ecol. Monogr.*, 86, 393–411.

Strona, G. & Fattorini, S. (2014). On the methods to assess significance in nestedness analyses. *Theory Biosci.*, 133, 179–186.

Strona, G., Galli, P., Seveso, D., Montano, S. & Fattorini, S. (2014). Nestedness for Dummies (NeD): a user-friendly web interface for exploratory nestedness analysis. *J. Stat. Softw.*, 59.

Swiecki, T.J. & Bernhardt, E. (2002). Evaluation of stem water potential and other tree and stand variables as risk factors for Phytophthora ramorum canker devel. *USDA Forest Service Gen. Tech. Rep. PSW-GTR-184*, 787–798.

Tooley, P.W. & Browning, M. (2009). Susceptibility to *Phytophthora ramorum* and Inoculum Production Potential of Some Common Eastern Forest Understory Plant Species. *Plant Dis.*, 93, 249–256.

Tooley, P.W., Browning, M. & Berner, D. (2008). Recovery of *Phytophthora ramorum* Following Exposure to Temperature Extremes. *Plant Dis.*, 92, 431–437.

Tooley, P.W., Browning, M. & Leighty, R.M. (2013). Inoculum Density Relationships for Infection of Some Eastern US Forest Species by *Phytophthora ramorum*. *J. Phytopathol.*, 161, 595–603.

Tooley, P.W., Kyde, K.L. & Englander, L. (2004). Susceptibility of Selected Ericaceous Ornamental Host Species to *Phytophthora ramorum*. *Plant Dis.*, 88, 993–999.

Valachovic, Y., Lee, C., Marshall, J. & Scanlon, H. (2008). Wildland management of Phytophthora ramorum in northern California forests. In: *In: Frankel, Susan J.; Kliejunas, John T.; Palmieri, Katharine M., tech. coords. 2008. Proceedings of the sudden oak death third science symposium. Gen. Tech. Rep. PSW-GTR-214. Albany, CA: US Department of Agriculture, Forest Service, Pacific Southwest Research Station. pp. 305-312.* fs.usda.gov.

Vaz, V.C., D'Andrea, P.S. & Jansen, A.M. (2007). Effects of habitat fragmentation on wild mammal infection by Trypanosoma cruzi. *Parasitology*, 134, 1785–1793.

Vehtari, A., Gelman, A. & Gabry, J. (2017). Practical Bayesian model evaluation using leave-one-out cross-validation and WAIC. *Stat. Comput.*, 27, 1413–1432.

Vehtari, A., Gelman, A., Simpson, D., Carpenter, B. & Bürkner, P.-C. (2020). Rank-Normalization, Folding, and Localization: An Improved $\widehat{R}$ for Assessing Convergence of MCMC. *Bayesian Anal.*

Vettraino, A.M., Hüberli, D. & Garbelotto, M. (2008). *Phytophthora ramorum* infection of coast live oak leaves in Californian forests and its capacity to sporulate *in vitro*. *Australas. Plant Pathol.*, 37, 72–73.

Wickham, H. (2016). *ggplot2: Elegant Graphics for Data Analysis*. Springer.

Wickham, H., François, R., Henry, L. & Müller, K. (2021). dplyr: A Grammar of Data Manipulation.

Widmer, T.L. (2015). Differences in Virulence and Sporulation of Phytophthora kernoviae Isolates Originating From Two Distinct Geographical Regions. *Plant Dis.*, 99, 460–466.

Wilber, M.Q., Johnson, P.T.J. & Briggs, C.J. (2020). Disease hotspots or hot species? Infection dynamics in multi-host metacommunities controlled by species identity, not source location. *Ecol. Lett.*, 23, 1201–1211.

Wilke, C.O. (2019). *cowplot: Streamlined Plot Theme and Plot Annotations for 'ggplot2'*.

Wojdak, J.M., Edman, R.M., Wyderko, J.A., Zemmer, S.A. & Belden, L.K. (2014). Host Density and Competency Determine the Effects of Host Diversity on Trematode Parasite Infection. *PLoS One*, 9, 10.

Woolhouse, M.E.J. (2001). Population Biology of Multihost Pathogens. *Science*, 292, 1109–1112.

Yao, Y., Vehtari, A., Simpson, D. & Gelman, A. (2017). Using Stacking to Average Bayesian Predictive Distributions. *Bayesian Analysis*, 13, 917–1007.

Young, H.S., Dirzo, R., Helgen, K.M., McCauley, D.J., Billeter, S.A. & Kosoy, M.Y. *et al.* (2014). Declines in large wildlife increase landscape-level prevalence of rodent-borne disease in Africa.

Proc. Natl. Acad. Sci. U.S.A., 111, 7036–7041.

Zhu, Y., Chen, H., Fan, J., Wang, Y., Li, Y. & Chen, J. *et al.* (2000). Genetic diversity and disease control in rice. *Nature*, 406, 718–722.